

1 TITLE:

2 How to determine microbial lag phase duration?

3

4 AUTHORS:

5 Monika Opalek^{1+*}, Bogna J. Smug^{2+*}, Dominika Wloch-Salamon¹

6 ¹ Institute of Environmental Sciences, Faculty of Biology, Jagiellonian University, Krakow, Poland

7 ² Malopolska Centre of Biotechnology, Jagiellonian University, Kraków, Poland

8 ⁺ These authors contributed equally to this work and share the first authorship

9 ^{*} Correspondence authors monika.opalek@doctoral.uj.edu.pl & bogna.smug@uj.edu.pl

10

11 KEYWORDS: lag phase length, microbial growth curve, fitness, lag time, bacterial growth models

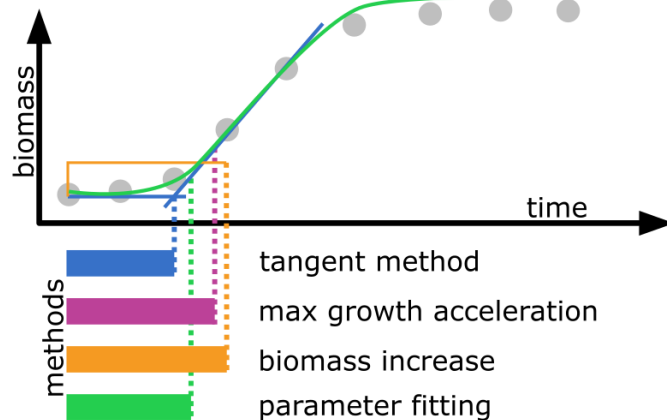
12

13 GRAPHICAL ABSTRACT

14

15

WHAT IS THE LAG PHASE DURATION?



microbial
lag phase
calculator



16 ABSTRACT

17 The lag phase is a temporary non-replicative period observed when a microbial population is
18 introduced to a new nutrient-rich environment. Its duration can have a pronounced effect on
19 population fitness, and it is often measured in laboratory conditions. However, calculating the lag
20 phase length may be challenging and method and parameters dependent. Moreover, the details of these
21 methods and parameters used throughout experimental studies are often under-reported. Here we
22 discuss the most frequently used methods in experimental and theoretical studies, and we point out
23 some inconsistencies between them. Using experimental and simulated data we study the performance
24 of these methods depending on the frequency of population size measurements, and parameters
25 determining the growth curve shape, such as growth rate. It turns out that the sensitivity to each of
26 these parameters depends on the lag calculation methods. For example, lag duration calculation by
27 parameter fitting to a logistic model is very robust to low frequency of measurements, but it may be
28 highly biased for growth curves with low growth rate. On the contrary, the method based on finding
29 the point where growth acceleration is the highest, is robust to low growth rate, but highly sensitive to
30 low frequency of measurements and the level of noise in the data. Based on our results, we propose a
31 decision tree to choose a method most suited to one's data. Finally, we developed a web tool where the
32 lag duration can be calculated based on the user-specified growth curve data, and for various explicitly
33 specified methods, parameters, and data pre-processing techniques.

34

35

36 INTRODUCTION

37 Microbial planktonic populations grown in a batch culture follow a predictable pattern in terms of how
38 the population size changes in time. Such growth kinetics can be represented by a growth curve which
39 is typically divided into the following phases: (1) lag phase, when cells adjust to a new environment
40 before they start dividing, (2) exponentially growing phase (or logarithmical growth), when cells
41 divide with a maximum rate and population's density doubles regularly, (3) stationary phase, when
42 cells cease divisions due to nutrients depletion, and, if the measurements are conducted long enough,
43 (4) the decline/death phase when population's density drops due to the cell death. Such pattern of
44 growth is typical for planktonic prokaryotic and eukaryotic microorganisms.

45 The lag phase was first described in 1895 by Müller as a temporary non-replicative period after
46 bacteria are introduced to new media [1]. Indeed, adjustment to a new environment after growth-arrest
47 requires broad cellular reorganizations, which are universal for prokaryotes and eukaryotes. The cells
48 need to adjust their transcriptome, and proteome (e.g. in *S.cerevisiae* [2–4]) and rearrange cellular
49 components that are necessary for nutrient uptake and biomass accumulation. These processes are
50 activated shortly after environment change - for example, it was reported that gene expression in
51 *Salmonella enterica* bacteria was affected as soon as 4 minutes after transfer into a fresh media, and
52 within 20 minutes, almost a thousand genes were upregulated [5]. Proliferation restart requires
53 induction of a broad range of processes, which include: glycolysis, nutrient sensing, amino acid
54 metabolism, nucleotide biosynthesis, protein processing (including translation, folding, modification,
55 translocation, and degradation), coenzyme and cell wall biosynthesis, transcription of genes involved
56 in stress response, respiration, cell cycle control, and division. For more details about biological
57 processes during the lag please see the review by Bertrand (2019) [6].

58 While many studies focus on the exponential phase and use the exponential growth rate as a measure
59 of population fitness [7], the quantification of the lag duration is equally important to assess the stress
60 or fitness of microbial populations [8,9]. Classically, fitness is defined by the number of progeny,
61 which in microbiology is translated into the growth rate (i.e. the rate at which the population size
62 doubles). However, the lag phase duration also affects fitness because it shows how quickly a given
63 cell or population can adapt to an environmental change. Shorter lags enable earlier divisions, which
64 might allow a cell to produce higher number of progeny within a fixed period of time. Such growth
65 dynamics would be especially important in case of competition for limited resources or a limited time
66 frame when resources can be used. Thus, the short lag phase is generally believed to be beneficial, and
67 therefore populations in favourable conditions may be expected to evolve toward decreased lag
68 duration [10]. However, the opposite strategy was observed in presence of antibiotics. In particular,
69 when bacterial populations were exposed to antibiotics before a transfer to new growth media, they
70 evolved towards increased lag duration which matched the duration of antibiotic exposure [11].

71 The variation in lag phase duration can be influenced by genetic, epigenetic, and environmental factors
72 (e.g. [12–14]). For *Saccharomyces cerevisiae*, both nuclear and mitochondrial genes are important
73 during the lag phase, and their expression patterns correlate with the lag phase length [13]. Besides
74 genetics, it has been shown that the lag phase duration is history-dependent. Namely, previous cells’
75 exposure to given conditions shortens the time needed to adapt if the conditions are reintroduced [14–
76 17]. What’s even more interesting - this effect has also been observed in daughter cells that had never
77 experienced the initially introduced conditions what suggests epigenetic inheritance. [15]. Lags of
78 individual cells may differ even within a clonal population grown in unaltered conditions. For
79 example, older cells experience longer lags than their younger clones [18,19]. Such heterogeneity may
80 be beneficial for the population, as it enables a bet-hedging strategy where a fraction of cells assures
81 fitness advantage by fast growth in favourable conditions, while the other fraction provides survival in
82 stressful conditions by extending their lag time [19–21].

83 There are multiple definitions of the lag phase and multiple ways of measuring its duration. One
84 common definition is based on microscopic observations and it uses the first morphological signs of
85 cell division as markers of the lag phase end (e.g. [15,22,23]). Within the studies on population-level,
86 the lag phase can be defined as the time before any detectable increase in the cell abundance (biomass)
87 [19], or as the time delay before a population reaches exponential growth [5]. To measure how the
88 population’s density (cell abundance) changes in time standard laboratory methods can be used.
89 Usually, one of the following methods is applied: spectrophotometry, colony counting on agar plates
90 (CFU, Colony Forming Unit), and flow-cytometry. Viability counts (CFU) provide precise estimates
91 of cell abundance even in a small population, however, this technique is time-consuming, requires
92 previously determined culture dilutions, and is difficult to automatize and scale up. Nevertheless, due
93 to its high sensitivity, it’s broadly used in food safety control [24,25]. Flow cytometry has a broad
94 detection spectrum and it enables simultaneous measurements of various cell properties e.g. cell size
95 or DNA content [26]. Spectrophotometry (optical density (OD) or absorbance) has narrower detection
96 limits, but it is convenient, fast, cost-effective, and can be easily adapted for high-throughput testing
97 via automatic measurements in constant time intervals.

98 Spectrophotometry is currently the standard way of obtaining microbial growth curves. However, one
99 of its limitations is the fact that optical density is an indicator of biomass rather than cell counts
100 (discussed by Swinnen *et al.* (2004) and Rolfe *et al.* (2012) [5,27]). To add to this problem, the optical
101 density may be also affected by dead or lysed cells, or even by the cell shape which may change
102 during the lag phase [28]. Additionally, if the inoculum size is small, exponential growth may start
103 before the biomass reaches the OD detection level, and thus the observed (apparent) lag duration may
104 be overestimated. This problem has been tackled by Baranyi (1999) [29] who proposed a so-called
105 time to detection (TTD) method which has been applied in some experimental studies (e.g. [30]). The
106 problem of initial biomass being below the detection level has also been tackled by Pierantoni *et al.*

107 (2019) [31] who have proposed a new calculation method that uses the apparent lag phases to measure
108 the initial population biomass. More broadly, the problem of density-based detection of growth for
109 small populations could be mitigated by assuming certain model growth curve shapes below the OD
110 detection level and/or by knowing the exact starting density of cells capable to proliferate (excluding
111 dead and senescent cells) [32].

112 Mathematical models can be used to overcome some methodological limitations. In order to know
113 when exactly cells started duplicating (i.e. the end of the lag phase), we would need to continuously
114 monitor the number of cells. This is, however, not possible with methods such as spectrophotometry.
115 As outlined above, the spectrophotometry measurements not only are taken in intervals, but also may
116 be inaccurate if the cells change their mass or shape, or if their initial amount is below the detection
117 level [5]. In such cases, some assumptions are needed to calculate the lag phase duration with
118 sufficient accuracy. If one assumes that there is no population growth during the lag phase and then
119 cells start synchronically dividing at a constant growth rate, the end of the lag phase can be calculated
120 as the intersection between the tangent line to the point of maximum growth rate and the $y = \log(N_0)$
121 line, where N_0 is the inoculation density (hereinafter “tangent method” [6]; see for example:
122 [12,15,24]). This is in fact the most frequently used method of calculating the lag duration. However,
123 there are also other methods, for example: defining the end of lag as the point of the growth curve
124 where the second derivative of the population size in time is maximal (hereinafter “max growth
125 acceleration”, e.g. [33,34]), determining when the biomass increased from the initial value by some
126 predefined threshold (minimal detectable increase, hereinafter “biomass increase”, e.g. [19]), or fitting
127 experimental data to a mathematical model (hereinafter “parameter fitting to a model”, e.g. [8]).

128 Various mathematical models have been proposed to account for the lag phase [27], and there are tools
129 and packages which use those to estimate the lag duration from the experimental data (for example R
130 package *nlsMicrobio* [35]). However, none of these tools is strictly focused on calculating the
131 population lag duration. Moreover, they require a good knowledge of the models and R programming
132 skills, which may make them difficult to use. Finally, as discussed in Baty *et al.* (2004) [32], the data
133 quality impacts the lag duration measurements to a higher extent than the choice of a model. Although
134 Baty *et al.* (2004) [32] investigated the insufficient number of data points as a potential problem in lag
135 duration calculation, experimental biologists may face other problems with the data quality such as
136 noisiness or growth curve shape that deviates from mathematical models [36]. Interestingly,
137 technicalities related to dealing with such ‘unideal’ data tend to be omitted in methodologies described
138 by empirical studies that measure lags. They have also not been discussed in theoretical studies which
139 focus on the mathematical formulations and biological assumptions rather than the reality and
140 limitations of laboratory experiments. These facts make a knowledge transfer between theoretical and
141 experimental biologists difficult.

142 Within this study, we describe the methods most frequently used to measure the lag duration and
143 discuss how these methods stem from various mathematical models describing microbial growth
144 curves. We highlight the advantages and limitations of each lag calculating method. We further use
145 both empirical and simulated growth curve data to show how the lag duration estimate may depend on
146 the data quality (i.e. noisiness), the shape of the growth curve, and the lag duration calculation method.
147 We propose a decision tree that may be useful in choosing the lag calculating method best suited to
148 one's data. We aim to emphasise that chosen methodology, parameters, and data pre-processing can
149 strongly influence the results, which is especially visible for less typically shaped growth curves.
150 Finally, we develop a publicly available web server MICROBIAL LAG PHASE DURATION
151 CALCULATOR (https://microbialgrowth.shinyapps.io/lag_calculator/) which allows calculating the
152 population lag duration according to various state-of-art methods. The calculator allows for fast and
153 easy data analysis and direct comparison of different methods.

154

155 THE LAG PHASE IN MATHEMATICAL MODELS

156 There are many mathematical models that describe the microbial population growth depicted by a
157 growth curve. They include the traditional simple models such as exponential [37], logistic [38] or
158 Monod growth [39], as well as more modern stochastic or agent-based models (see the review by
159 Charlebois and Balázsi (2019) [40]). While the pure exponential model is parametrised only by the
160 *growth rate*, the other models may depend on multiple parameters. For example, the logistic model
161 introduces the *carrying capacity* parameter which represents the maximum population size, and
162 Monod model introduces the so-called *half-velocity constant* (which quantifies the relationship
163 between nutrient concentration in media and population growth rate). Another version of this model
164 may be parametrised by the *maximum resource uptake rate* and the *saturation constant* as derived by
165 Michaelis-Menten.

166 Please note, that within this publication „method” refers to the way in which the lag phase is
167 determined, while “model” refers to a set of equations that reproduce the entire microbial growth
168 curve.

169 Out of the three typically described growth phases (lag, exponential and stationary phase), the
170 exponential and stationary phases are recovered by most of the models discussed in Charlebois *et al.*
171 (2019) [40]. One exception is the pure exponential model which only describes the exponential phase.
172 However, the lag and death phases require additional assumptions and are rarely described with
173 sufficient detail. The models that aim to capture or predict the lag phase are well summarised in the
174 two extensive reviews [27,32]. Some models describe the lag only phenomenologically. For example,
175 the Baranyi (1993) and Baranyi and Roberts (1994) [41,42] models assume that there is some
176 adjustment function that describes the population's adaptation to a new condition. On the other hand,
177 there are models that attempt to make specific assumptions regarding what happens in the lag phase.
178 The Hills and Wright (1994) [43] assume that certain biomass needs to be reached for the cell to start
179 the chromosomal replication. Consequently, their model independently tracks in time the amount of
180 biomass and chromosomal material. The model proposed by McKellar (1997) [44] assumes there is
181 some heterogeneity in the population, and that one part of the population grows exponentially from the
182 very beginning, whereas the other part does not replicate. A more realistic version of this model was
183 proposed by Baranyi (1998) [45] where the non-replicating cells are assumed to transform at a
184 constant rate into the replicating ones, meaning that they exit the lag phase. Finally, a model by Yates
185 (2007) [46] adds another compartment, namely cells that die at a constant rate. This specific
186 assumption allowed the model to reproduce the initial biomass decline which is sometimes observed
187 during the lag phase. Interestingly, as noticed by Baty (2004) [32], some of the models described
188 above are equivalent, in spite of being based on distinct biological assumptions.

189

190 THE LAG PHASE CALCULATION METHODS

191 The most popular and intuitive method of calculating the lag duration ("tangent method") defines the
192 lag phase end at the intersection point of $\log(N_0)$ (where N_0 denotes the initial biomass) and a line
193 tangent to the logarithm of population size in the exponential phase [6,39]. Why bother about more
194 complicated mathematical models?

195 The definition above is in fact a consequence of the pure exponential growth assumption. If cells do
196 not divide for some time λ and then start growing with a constant growth rate, then the time λ perfectly
197 corresponds to the lag as measured by the intersection between the lines described above (Table 1, Fig.
198 1: exponential model & tangent method).

199 However, microbial populations in a batch culture do not grow with a constant growth rate. According
200 to the Monod model assumptions [39], the growth rate depends on the availability of the resources,
201 and therefore it decreases over time. The growth rate may also depend on other factors, e.g. the
202 population density [47]. In the case of cancer cells or in populations that reproduce sexually the
203 growth rate may be lower at low population density, which is known as the Allee effect (e.g. [48,49]).

204 This is why, in order to assess the most exact time when cells start divisions, there is a need for a
205 mathematical model that is likely to represent the empirical growth curve and to fit the lag time
206 together with other growth parameters. In particular, note that when there is some growth detection
207 threshold, the time by which we notice any growth (i.e. apparent lag) may be impacted not only by the
208 lag length but also by other growth parameters. For example, when the initial biomass and growth
209 rates are very low, the slow growth may not be detected and treated as lag. This problem has been
210 extensively discussed in Pierantoni *et al* (2019) [31].

211 The summary of the most popular methods of calculating the lag duration, the assumptions underlying
212 each of the methods as well as possible challenges related to each method are given in Table 1.

213

Name	Lag end calculation method	Underlying model assumptions	Challenges	Example data for which the method is suitable	Examples of experimental studies using the method
BIOMASS INCREASE	The increase of OD or biomass by a certain value from the beginning of the growth.	The population size does not increase its biomass during the lag and then starts growing with any growth rate that may be variable or hard to measure. The increase by the threshold value is the minimal increase possible to detect with high confidence.	Choice of the threshold value is arbitrary (not 'biologically- relevant')	Data where the initial size of the viable population cannot be determined with high confidence.	Opalek <i>et al.</i> 2022 [19]
MAX GROWTH ACCELERATION	The point of the growth curve where the second derivative of population size in time is maximal.	The population size does not increase its biomass during the lag and then starts growing with a decreasing growth rate.	Noisy data may affect the detection of such a point.	Growth in a batch culture where the amount of resources decreases with time and the amount of unfavourable by-products increases with time.	Liu <i>et al.</i> 2021 [33]
TANGENT METHOD	The intersection of the initial density line and the line tangent to the growth curve at the maximal growth rate (on log. scale).	The population size does not increase its biomass during the lag and then starts growing exponentially with a constant growth rate.	If the growth rate varies, it may be challenging to find the "real" or maximal growth rate. Moreover, the initial density needs to be determined with high confidence	Growth in constant resources and environmental conditions (e.g. chemostat (at starting point), serial transfers).	Valík <i>et al.</i> 2021 [24]
PARAMETER FITTING TO THE BARANYI MODEL	Using parameter fitting procedures in order to simultaneously find all Baranyi & Roberts model parameters that provide the best fit to the entire growth curve. Then the lag is defined as $\ln(1 + 1/q_0)/r$ where r is the maximal growth rate and q_0 represents the physiological state of the inoculum.	The population size grows according to the logistic model adjusted by function: $\alpha = q(t)/(1 + q(t))$ where $q(t) = q_0 e^{vt}$ describes the concentration of some critical substance. The adjustment function slows down the initial growth but it does not pause it during the lag time as assumed by other methods.	The lag duration fitted to the data may depend on many technical parameters of the fitting algorithms, or it may not be found if the fitting algorithms fail to converge. Finally, the lag understood by Baranyi is not the time when cells do not divide, but the time required to adjust to the new media (see Discussion for more details)	Data that is well described by the Baranyi & Roberts model, where ideally some parameters (r , K , or q_0) are known <i>a priori</i> .	Kim <i>et al.</i> 2022 [50]
PARAMETER FITTING TO THE LOGISTIC MODEL	Using parameter fitting procedures in order to simultaneously estimate the lag duration, carrying capacity, and growth rate parameter values.	The population size does not increase during the lag and then starts growing according to the logistic model: i.e. with the growth rate decreasing according to the following equation: $r(1-N(t)/K)$ where r is the maximal growth rate, K is the maximal population size, and $N(t)$ is the population size at time t .	Assumes a very specific growth curve shape. Moreover, the lag duration fitted to the data may depend on many technical parameters of the fitting algorithms. Finally, the fitting methods may not converge to any solution.	Data that is well described by the logistic model, where ideally some parameters (r or K) are known <i>a priori</i> .	Reding-Roman <i>et al.</i> 2017 [8]

215 RESULTS

216 TESTING METHODS FOR LAG DURATION DETERMINATION ON THE SIMULATED DATASET

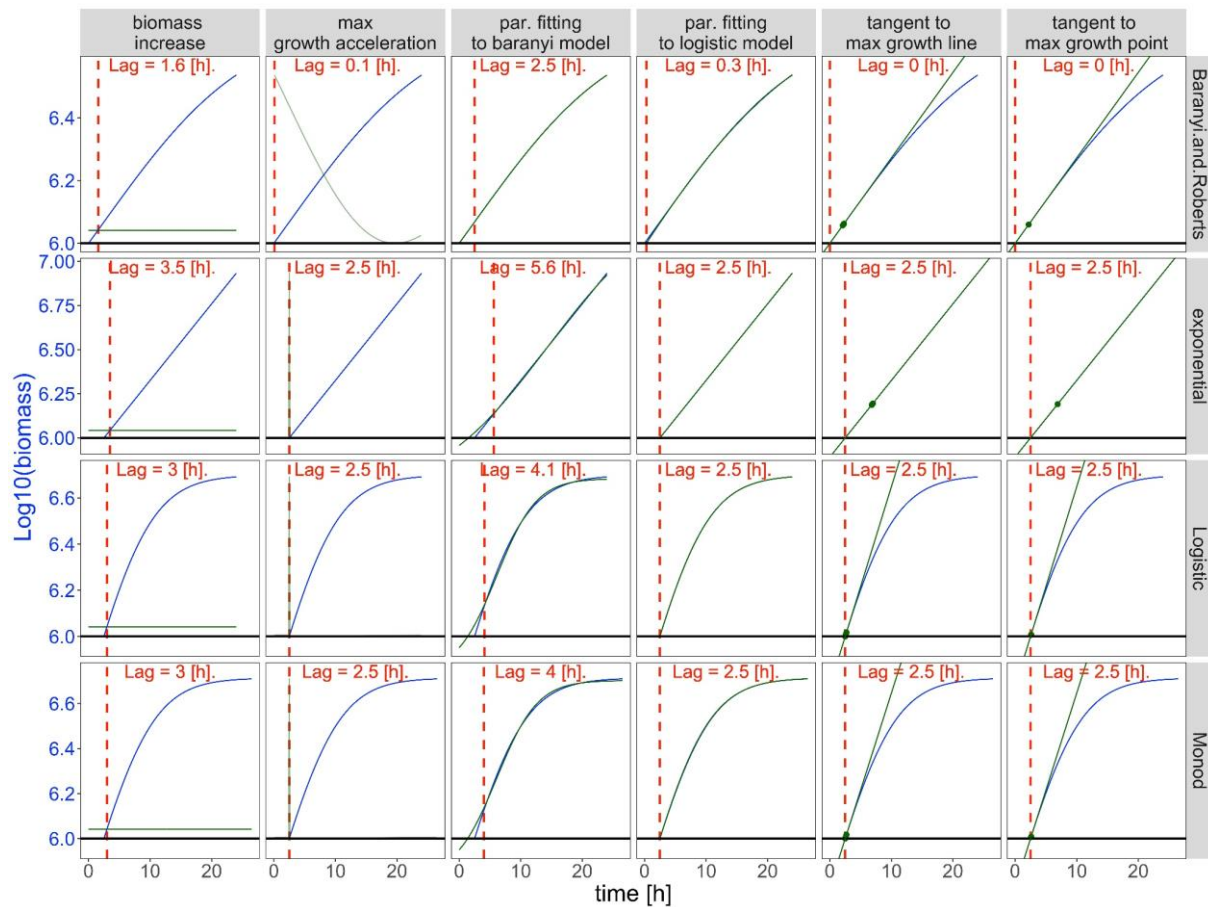
217 Given that the methods of calculating the lag phase duration described above (Table 1) were based on
218 theoretical assumptions, we first simulated microbial growth curves based on various well-known
219 deterministic mathematical models: (i) the simple EXPONENTIAL model which assumes that microbes
220 do not grow nor divide for some time (lag) and then start growing exponentially with a constant
221 growth rate; (ii) LOGISTIC model which assumes the microbes do not grow nor divide for some time
222 (lag) and then start growing exponentially with a decreasing growth rate; (iii) MONOD model where
223 microbes do not grow nor divide for some time (lag) and then the speed of the growth after the lag
224 phase is coupled with the decrease in resources, and (iv) BARANYI model which assumes cells do
225 grow and divide in the lag phase but that growth is slower than in the exponential phase. See the
226 Appendix for the formulation of each model. We set that for all generated growth curves the lag phase
227 lasts for 2.5 hours.

228 Then, for each of these simulated growth curves, we calculated the lag phase duration using the well-
229 established methods described in Table 1. The most common tangent method was further split into:
230 tangent to point (i.e. where the tangent line is drawn to the first point where the growth rate is
231 maximal) [23] and tangent to line method (i.e. where the tangent line is understood as a regression line
232 fitted to a number of points around those with the maximal growth rate) [7].

233 Max growth acceleration, parameter fitting to the logistic model, and both tangent methods found the
234 correct lags (lag = 2.5 h) for data simulated under exponential, logistic, and Monod models (Fig. 1).
235 Even the simplest tangent method worked well for the data simulated under these models, even though
236 the data does not necessarily meet the assumption of a constant growth rate. Importantly the Baranyi
237 model seems to be inconsistent with all other models. Namely, the lag durations calculated for the data
238 simulated under the Baranyi model are underestimated by all methods apart from the one where
239 parameters are fitted explicitly to the Baranyi model. Conversely, the parameter fitting to the Baranyi
240 model method tends to overestimate the lags for data simulated under all models apart from Baranyi.
241 The biomass increase method overestimates lag phase duration by one timepoint (0.5 h) for logistic
242 and Monod models and two timepoints (1 h) for the exponential model. It is the consequence of this
243 method formulation, where lag phase end is defined as the first timepoint after detectable growth.

244

245



246

247 Fig. 1. Lag phase durations (given in red) calculated for data (blue lines) simulated under various
 248 models (rows) and calculated by different methods (columns). The red dashed lines indicate the end of
 249 the lag phase, black solid lines indicate the initial biomass (first measurement) and the green lines are
 250 (left to right): the threshold of log(biomass) value at which the lag phase is assumed to end [biomass
 251 increase method]; second derivative of log(biomass) scaled to the values visualised in the plot [max.
 252 growth acceleration method]; fitted growth curve [par. fitting to the Baranyi model and par. fitting to
 253 logistic model methods]; tangent lines to the exponential growth [tangent to max. growth line and
 254 point methods].

255

256

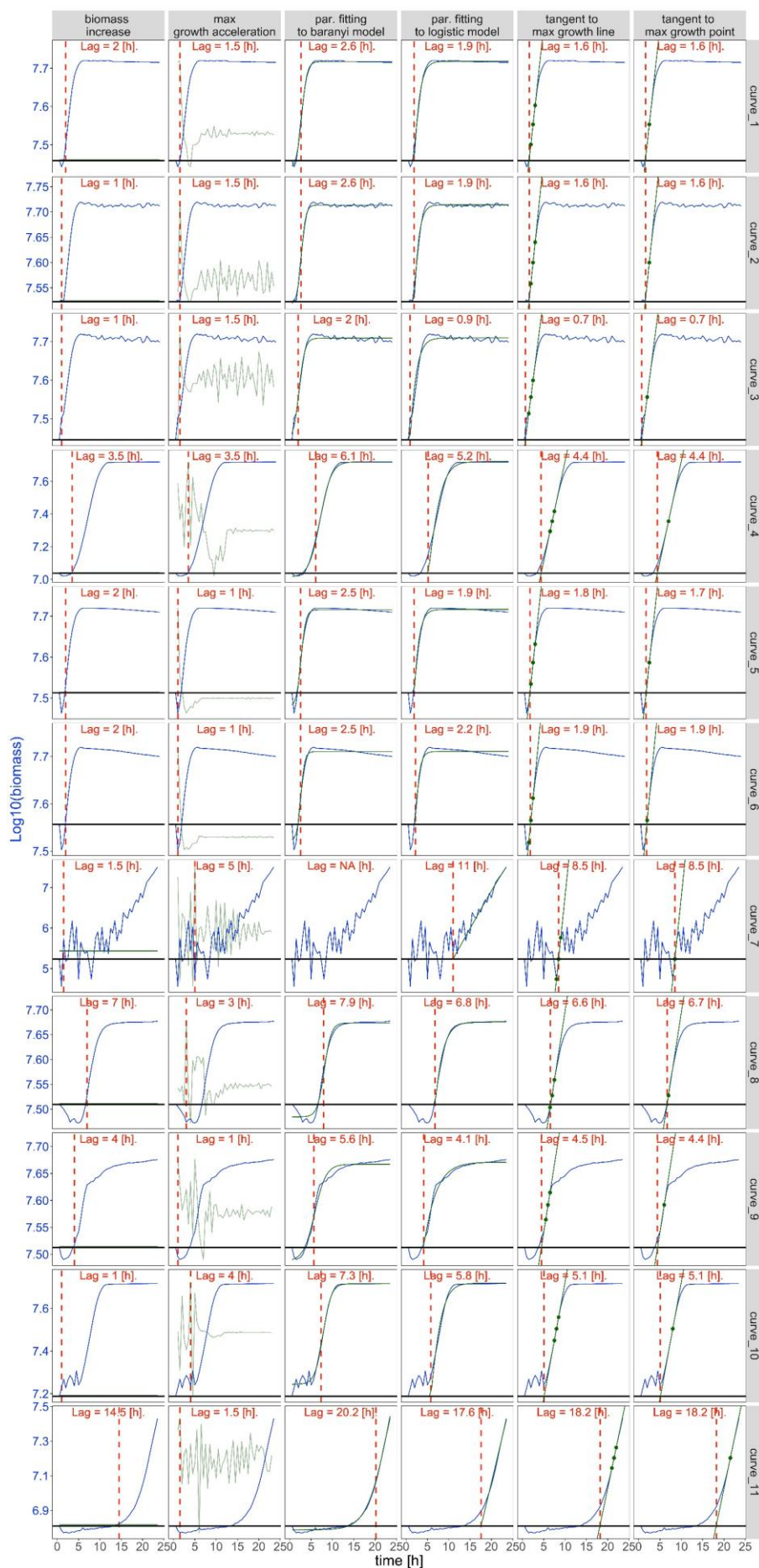
257

258 TESTING METHODS FOR LAG DURATION DETERMINATION ON THE EMPIRICAL DATASET

259 Having verified how the lag calculation methods work on simulated data (Fig. 1), we set off to verify
260 how these methods perform on real experimental data. We used 11 growth curves from
261 *Saccharomyces cerevisiae* grown in various conditions (see Methods and Supplement). Some of these
262 curves resemble the model data, while others are much noisier and challenge some of the model
263 assumptions, for example: the biomass drops at the beginning of measurements (Fig. 2: curve_5 and
264 curve_6), there is no typical exponential phase (Fig. 2: curve_11) or the lag phase is boldly prolonged
265 and turbulent (Fig. 2: curve_7 and curve_11). Results obtained for empirical data show that the lag
266 duration estimates may vary depending on the lag calculation method (Fig. 2, Supplementary Table 2).
267 The lowest discrepancy between different methods is observed for curve_1, where the lag duration
268 calculated by all methods is 1.86 ± 0.83 h. In some cases, all but one method give similar results (e.g.
269 curve_7, where the biomass increase method gives an outlying result), in others, some methods fail to
270 find the correct lag duration (e.g. curve_7, curve_11) due to the data noisiness (Fig. 2). The highest
271 discrepancy between methods was obtained for curve_11 where a minimal lag phase length of 1.5 h
272 was obtained by the max growth acceleration method, while both tangent methods and parameter
273 fitting to logistic model yielded the lag duration of ~18h.

274

275



276 Fig. 2. Lag phase duration (given in red) calculated for empirical growth curves (blue lines) obtained
277 for *S. cerevisiae* grown in various conditions (top to bottom). The red dashed lines indicate the end of
278 the lag phase, black solid lines indicate the initial biomass (first measurement) and the green lines are
279 (left to right): threshold value at which the lag phase is assumed to end [biomass increase method];
280 second derivative of log(biomass) scaled to the values visualised in the plot [max. growth acceleration
281 method]; fitted growth curve [par. fitting to Baranyi model and par. fitting to logistic model methods];
282 tangent lines to the exponential growth [tangent to max. growth line and point methods].

283

284

285 TESTING THE SENSITIVITY OF LAG DETERMINATION METHODS TO DATA NOISINESS

286 In order to understand the source of possible errors and biases in lag calculation on experimental data,
287 we simulated growth curves from the logistic model (which in our experience the most adequately
288 represents the real growth curves) and to each curve we added noise simulated from the random
289 distribution with mean = 0 and standard deviation dependent on the initial biomass B_0 (Supplementary
290 Fig. 2). Thus, our simulated growth curves could be described as:

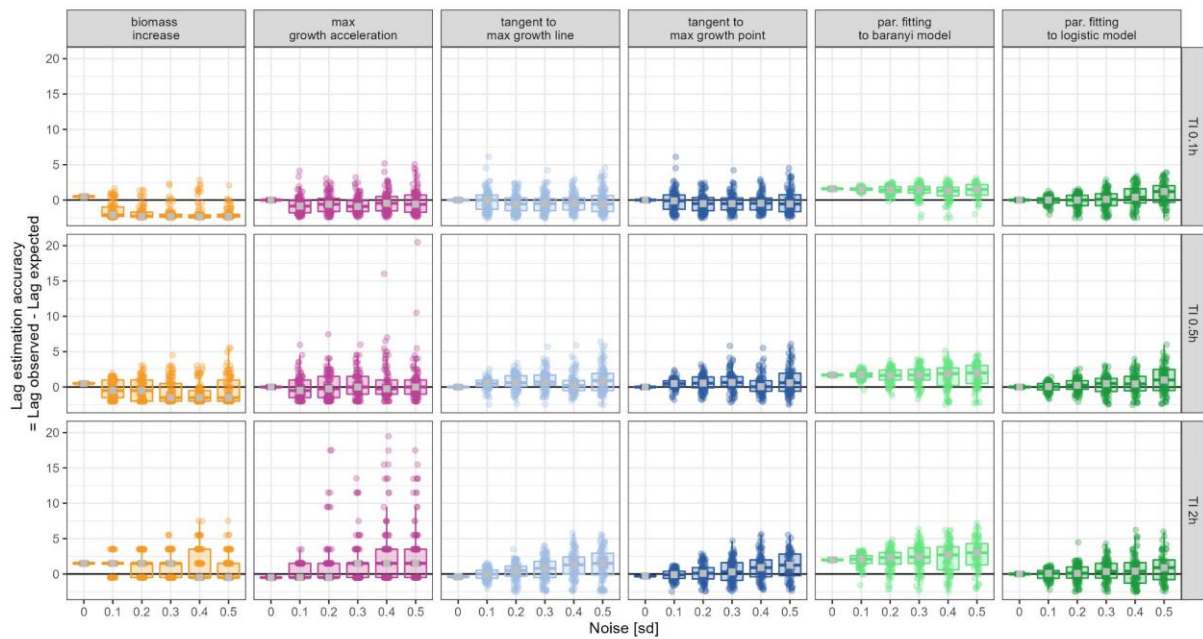
291 $B_{noisy}(t) = B(t) + N(0, sd * B(0))$, where $B(t)$ is the solution from the deterministic logistic model
292 with a lag component (see Supplement for the formulation of this model).

293 We varied the level of noisiness (i.e. set sd between 0 and 0.5) together with other parameters such as:
294 population growth rate, lag time, and time interval between data points (which represents the
295 frequency of population size measurements). For each combination, we simulated 100 curves. Then
296 for each of these curves, we calculated the lag according to each of the lag calculation methods and we
297 calculated the bias i.e. the difference between observed and expected lag.

298 First, we tested how the frequency of population size measurement impacts the lag estimation. In
299 agreement with previous reports [32], it turned out that frequent measurements improve the accuracy
300 of lag duration estimation. This effect can be observed within all lag calculation methods (Fig. 3: top
301 vs bottom row) and it is especially pronounced for data with high noise ($sd = 0.5$). Large time intervals
302 between data points (Fig. 3: bottom row) lead to increased variance in the lag duration estimation
303 (wide boxplot) and to high bias (median value deviates from $y = 0$ line). It is especially pronounced in
304 the biomass increase and max growth acceleration methods which overestimate lag durations even
305 when there is minimal amount of noise (low sd). Such bias results from the fact that these methods
306 operate only on the data points provided and they do not use any implicit models to interpolate
307 between them.

308

309



310

311 Fig. 3. The impact of time intervals (TI) between subsequent measurements of population size on lag
312 phase duration estimations. For each sd (noisiness, x-axis), measurement frequency (time interval,
313 rows), and lag calculation method (columns) 100 simulations were conducted (points). The y-axis
314 illustrates the difference between true (expected, set as 2.5 h) and estimated (observed) lag. Boxplots
315 illustrate the distribution of points, and the median value (grey square). All points located above $y = 0$,
316 show these calculations where lag phase length was overestimated, similarly, all points below $y = 0$
317 show calculations where lag duration was underestimated.

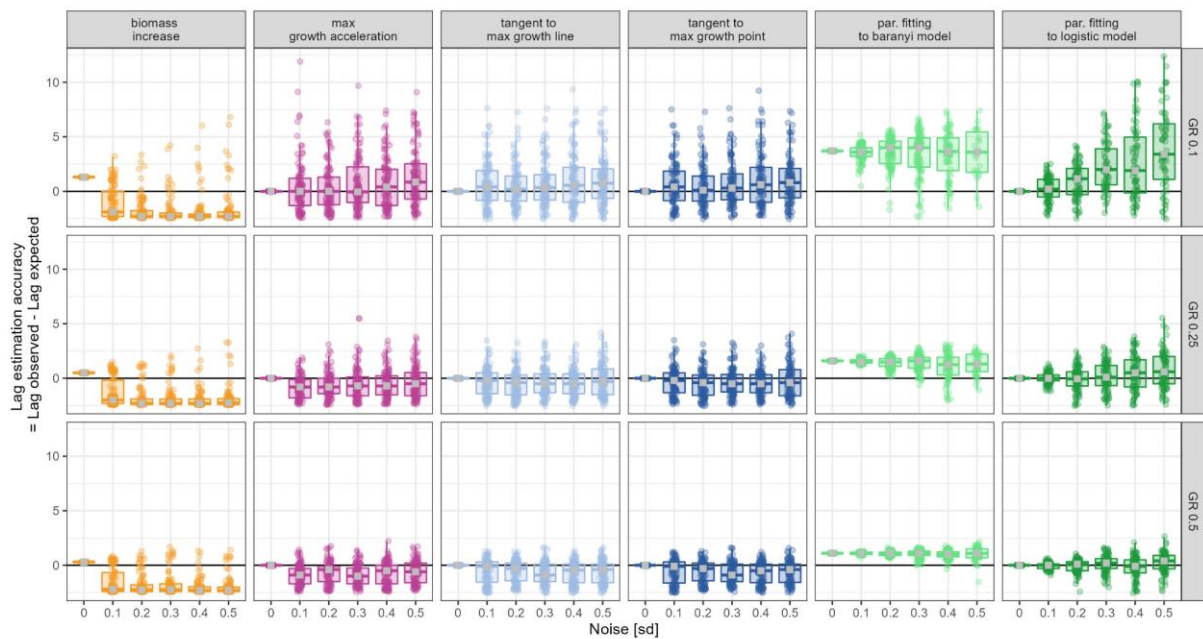
318

319 Next, we checked whether the population's growth rate has an impact on lag estimation. We calculated
320 lags for three growth rates representing slow, moderate, and fast growth, and for varied levels of data
321 noisiness (Fig. 4). For most of the methods slow growth results in low accuracy of lag estimation,
322 which may additionally decrease when data is noisy. These results are consistent with our experience,
323 namely, when the growth curve is flat, it is challenging to find a point where the population starts
324 growing exponentially (Fig. 4: top row). In contrast, even for noisy data, fast growth facilitates lag
325 phase estimations (Fig. 4: bottom row). The only method which is not affected by the growth rate is
326 the biomass increase method, however it systematically underestimates lag duration, and this bias
327 increases with introduced noisiness. Conversely, the parameter fitting to the Baranyi model
328 systematically overestimates lag lengths especially when the population grows slowly. Max growth
329 acceleration and both tangent methods are not biased, and are sensitive to growth rates to a similar
330 degree, where lag estimates become less accurate with increasing noise. Interestingly, parameter
331 fitting to the logistic model shows good accuracy and no bias for moderate and fast growth, but it
332 suffers from low accuracy and high bias in the case of low population growth rate and high levels of
333 noise.

334 Another factor that affects the lag length estimation accuracy is the actual length of the lag phase. The
335 longer the lag, the easier it is to erroneously detect some noise during the lag phase as the first signs of
336 growth. Indeed, if a population has a long lag phase, its duration tends to be underestimated, while
337 very short lags tend to be overestimated by all methods. This bias is increasing with higher noisiness
338 (Supplementary Fig. 3), with the estimations of lag phase duration by parameter fitting to the logistic
339 model being the most robust.

340

341



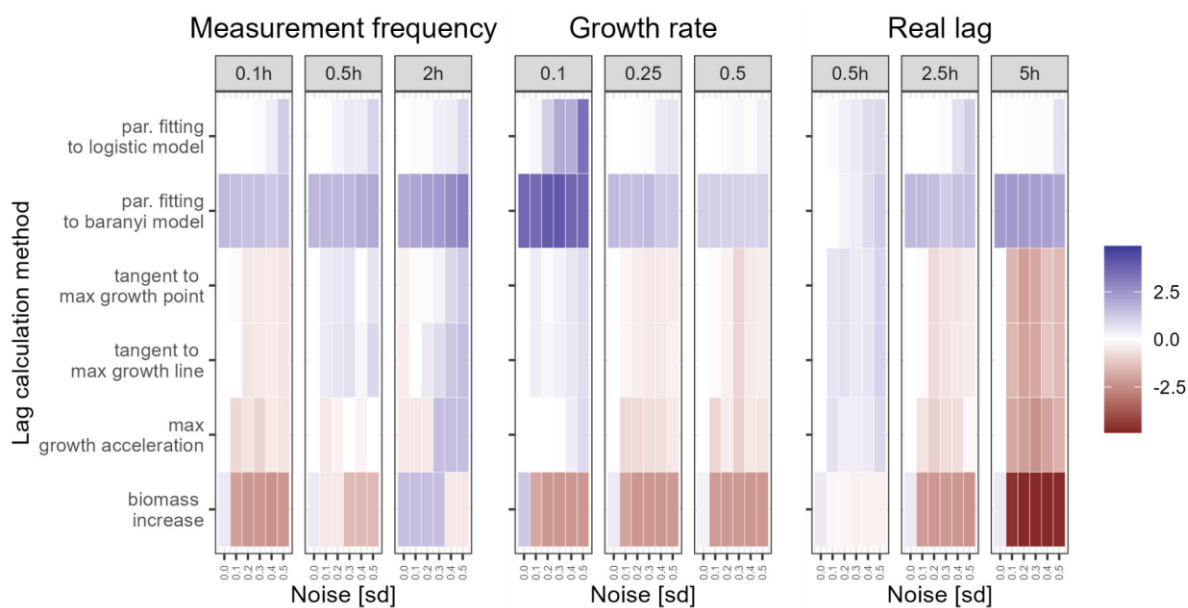
342 Fig. 4. Impact of growth rate (GR) on lag phase duration estimations. For each sd (noisiness, x-axis),
343 growth rate (rows), and lag calculation method (columns) 100 simulations were conducted (points).
344 The y-axis illustrates the difference between true (expected, set as 2.5 h) and estimated (observed) lag.
345 Boxplots illustrate the distribution of points, and the median value (grey square). All points located
346 above $y = 0$, show these calculations where lag phase length was overestimated, similarly, all points
347 below $y = 0$ show calculations where lag duration was underestimated.

348

349 The comparison of biases of all lag calculation methods are shown in Fig. 5. The methods that tend to
350 be systematically biased within our parameter range are the biomass increase (underestimates the lags)
351 and fitting to Baranyi model (overestimates the lags). The biomass increase tends to erroneously pick
352 random points as sudden lag phase end, which leads to underestimation of lag phase duration.
353 Conversely, the parameter fitting to the Baranyi model systematically overestimates lag duration. This
354 is a consequence of the dataset being simulated by the logistic model which is inconsistent with
355 Baranyi's assumptions. The other methods are less biased within our parameter range. Both tangent
356 and max growth acceleration methods have poor performance on growth curves with long lags, and
357 max growth acceleration method is very sensitive to high levels of noise. The parameter fitting to the
358 logistic model is the most robust to data noisiness, however, interestingly what affects it the most is
359 the low growth rate.

360

361



362

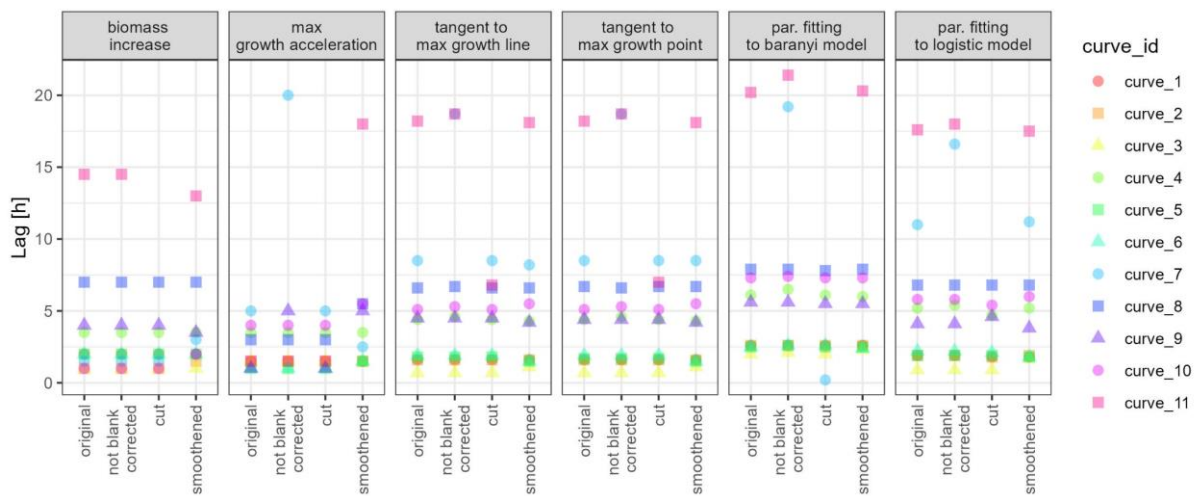
363 Fig. 5. The median bias of lag estimation of each of the lag calculation methods applied to growth
364 curves with varied level of noise (x-axis) and other growth curve parameters (column panels). White
365 squares mean the method is unbiased, blue means the lags tend to be overestimated, and red means the
366 lags tend to be underestimated.

367

368 TESTING THE EFFECTS OF DATA PRE-PROCESSING ON ESTIMATED LAG LENGTHS

369 Lag estimation is challenging if data is noisy. This problem could be mitigated by some data pre-
 370 processing techniques that allow for removing noise from the data. Therefore, we verified how manual
 371 curation or data pre-processing affect the lag calculation accuracy. We applied the following pre-
 372 processing methods to our experimental curves (Fig.2): (i) smoothing the curve by Tukey’s
 373 smoothing function, (ii) cutting the data at 12h to remove the noise observed in the stationary phase. It
 374 turned out that for the “typical” growth curve shapes, such as the ones presented in curve_1 and
 375 curve_2 (Fig. 2), various algorithms are consistent and the data pre-processing does not influence the
 376 results. However, the noisier the data, the less consistent the results based on multiple lag calculation
 377 methods and data pre-processing techniques (Fig. 3). We have additionally verified that adding a
 378 constant to the entire growth curve (e.g. by neglecting the blank correction) affects the lag phase
 379 length estimates given by all but the biomass increase method (Fig 3). Importantly, such a constant
 380 value added to the growth curve may not only relate to blank correction, but also to the case when a
 381 fraction of the population is dead or damaged and does not duplicate throughout the growth. We
 382 further investigate how that phenomenon affects the lag calculation in Supplementary Fig 1.

383



384

385 Fig. 6. Distribution of lag duration estimated by six discussed methods (columns) per each curve
 386 (colour & shape) and pre-processing algorithm (x-axis). “Original” means no pre-processing has been
 387 applied, “not blank corrected” means data were not corrected for the blank value, “cut” means the data
 388 curve has been shortened to 12 hours only, and “smoothed” means Tukey smoothing has been
 389 applied.

390

391

392 HOW TO CHOOSE THE LAG CALCULATION METHOD BEST SUITED TO ONE'S DATASET?

393 We propose a decision tree to facilitate the choice of lag calculation method (Fig. 7A). The
394 recommendations are based on our results shown in previous sections. Altogether, we suggest trying to
395 estimate lag duration by parameter fitting to the logistic model in the first place. This method is the
396 most robust, it captures whole growth dynamics and because of that, it mitigates technical limitations
397 (such as a device's detection limits). On the other hand, the biomass increase method is the least
398 dependent on any assumptions. In particular, it is the only one that is not affected by the blank
399 correction or existence of dead cells in the culture. Therefore we recommend it if the other methods
400 cannot be applied. Additionally, we encourage to use multiple methods and to investigate possible
401 inconsistencies between their results.

402

403

404 THE LAG PHASE DURATION CALCULATOR

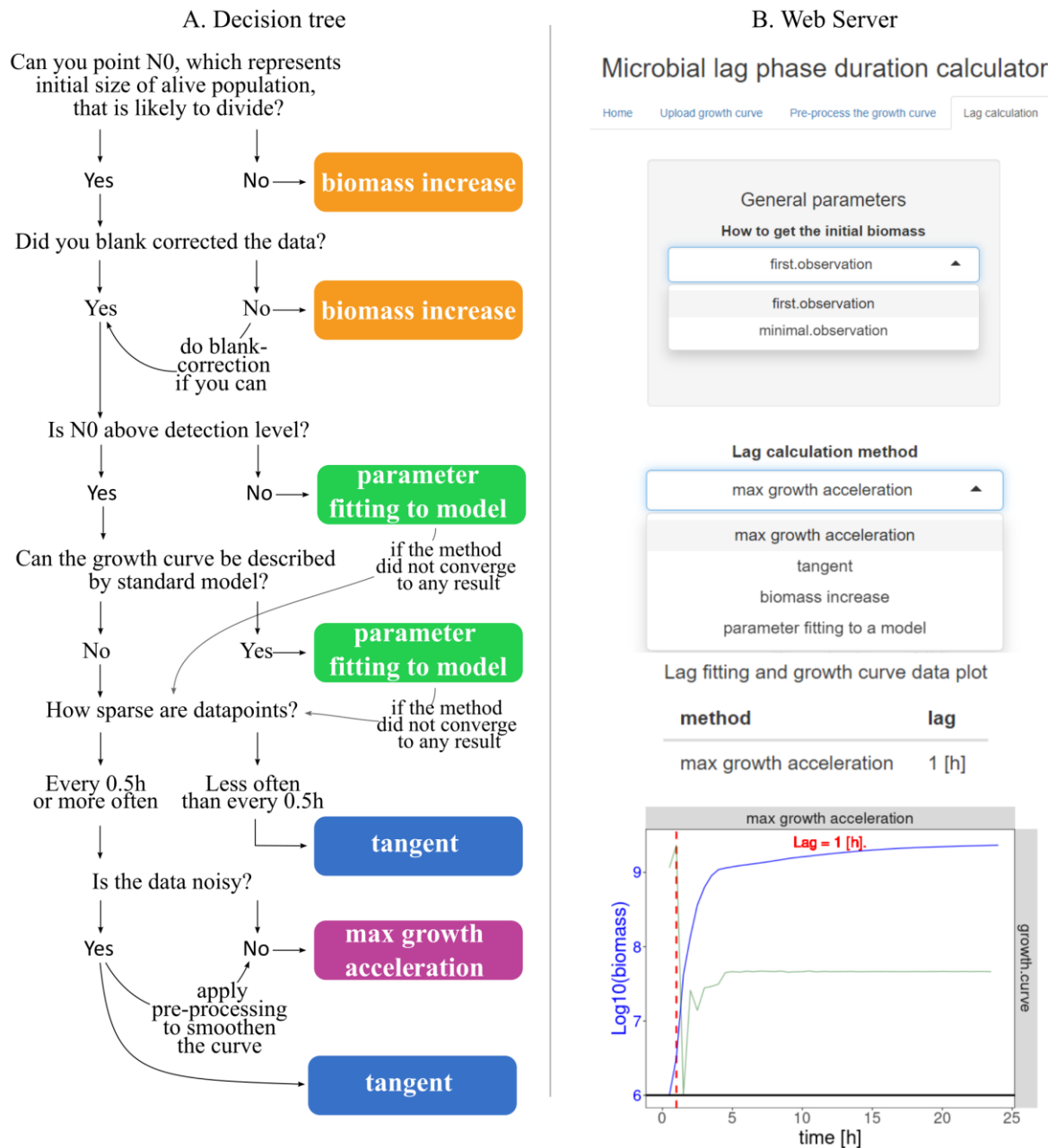
405 Finally, in order to allow other researchers to calculate lag duration by different methods and compare
406 the results, we created a web server MICROBIAL LAG PHASE DURATION CALCULATOR, where
407 lags can be calculated by various methods upon insertion of the growth curve data (i.e. table with time
408 and biomass columns). The webservice is freely available under the following address:

409 https://microbialgrowth.shinyapps.io/lag_calculator/

410 The MICROBIAL LAG PHASE DURATION CALCULATOR is designed to automate the lag
411 duration calculation process. The tool does not require any programming, nor mathematical modelling
412 skills. Additionally, we deposited our code and lag calculating functions on GitHub so that they can be
413 used locally, customised, and further improved.

414

415



416 Fig. 7. A: Decision tree to facilitate the choice of appropriate lag calculation method. B: Print-screen
 417 from web server MICROBIAL LAG PHASE DURATION CALCULATOR where lag phase duration
 418 can be calculated for a user-specified growth curve, and by any of the methods discussed in Table 1.

419 DISCUSSION

420 Lag phase duration is an important fitness component for microbial populations. Within this
421 publication, we discussed the most popular approaches to calculate the lag phase duration for
422 population-level data. We implemented these approaches and tested them on simulated and empirical
423 data to show that they may disagree depending on the shape of the growth curve. To further compare
424 the methods in terms of their accuracies and biases, we simulated growth curve data with varied level
425 of noise and other parameters such as growth rates, lag lengths or the time intervals between data
426 points (understood as the frequency of measurements). For each of these growth curves we estimated
427 the lag duration with each of the lag calculation methods. It turned out that the noise and other
428 parameters affect the quality of lag duration estimation, hence we tested how smoothing the growth
429 curve and other data pre-processing techniques influence the lag estimation. Since various methods
430 were sensitive to various parameters (for example the max. growth acceleration method was largely
431 affected by the high noise, while the parameter fitting to logistic model method was affected by low
432 growth rates), we used our results to propose a decision tree designed to help in choosing the lag
433 calculation method best suited to one's data. We have also developed a web tool where the lag duration
434 can be calculated based on the user-specified growth curve data, and for various explicitly specified
435 methods, parameters, and data pre-processing techniques. Additionally, we deposited our code on
436 GitHub so that the function “Calculate.Lag” can be taken directly to the R environment for local use
437 and customization.

438 Here, we chose the four most frequently used approaches to estimate lag phase duration. We compare:
439 (i) THE BIOMASS INCREASE, which uses a predefined value of a biomass (or absorbance) gain that can
440 be confidently marked as population's growth; (ii) THE MAX GROWTH ACCELERATION, which assumes
441 the lag ends at the time point where the second derivative of a population size in time is maximal, (iii)
442 THE TANGENT METHOD, where lag phase endpoint is marked as the intersection point of a line tangent
443 to maximal growth and a line $y = \log(N_0)$, where N_0 is population density at the inoculation; and (iv)
444 PARAMETER FITTING TO A MODEL which simultaneously finds best-fitted parameter values for the
445 entire curve (e.g. lag phase length, maximal population size, maximal growth rate) using logistic or
446 Baranyi models. All these methods are developed based on typically shaped growth curves. Therefore,
447 we tested the accuracy of their estimations using simulated (typical) and empirical (typical and
448 untypical) growth curve data. As expected, for data with typically shaped growth curves, the majority
449 of the methods showed similar results. This is in line with the previous observation, that the choice of
450 a model influences the calculated lag phase duration to a lesser extent than the data quality and
451 characteristic [32]. Interestingly the Baranyi model [51] is not consistent with other methods. This is a
452 consequence of how the lag is defined within Baranyi model. While other models assume the lag is the
453 time when the population size does not grow, Baranyi defines lag as the delay between the population
454 size expected if the cells started growing immediately after inoculation with the maximum growth rate

455 and the observed one [32]. This is consistent with the original definition [52] which defines lag
456 duration as the difference between the time expected to take to reach the observed population size if
457 population size was growing at a maximal rate and the actual time taken to reach that population size
458 (including the lag duration). Note, however, that such definition is affected by all factors that lead to a
459 slower growth (e.g. nutrient depletion), and may be dependent on the time when measurements are
460 taken.

461 Taken together, the lag phase estimation cause little or no trouble when the growth curve resembles a
462 standard model shape, and in such cases, the choice of the lag calculation method can be driven by
463 one's preferences. It, however, becomes more complicated for noisy or untypical growth curves.

464 In line with previous research [32], we demonstrated that the frequency of measurements can strongly
465 influence the lag phase duration estimates (Fig. 4). We recommend taking measurements with
466 maximal 0.5h intervals, and more frequently if one expects untypically shaped growth curves. We also
467 highlight the importance of correct calculation of N_0 (the initial number of alive cells, capable of
468 proliferating) and of that number being above the detection limit. In the laboratory settings, this
469 number can be relatively easily adjusted by adequate dilutions and simultaneously gives a much
470 broader spectrum of possible analysis afterward. If N_0 is below the detection level, then we are likely
471 to overestimate the lag duration, because the first signals of growth will also be under detection level.
472 To overcome this problem, one can assume a certain growth curve shape below the detection limit as
473 done in Pierantoni *et al.* 2019 [31] and apply model fitting to estimate the lag duration. Additionally, if
474 this number cannot be measured with high confidence (for example because of some dead or senescent
475 cells being a part of the inoculum) one can use the biomass increase method to estimate population lag
476 duration.

477 Although THE BIOMASS INCREASE method is simplistic, and it may be questionable if its results
478 represent the real lag length, we believe it provides a good ecological measure of how efficiently a
479 given population can inhabit a niche (net biomass gain). We suggest to apply this method if the growth
480 curve greatly deviates from model shape or when the growth curve cannot be corrected for blanks or
481 dead cells (i.e. if a fraction of the population size accounts for dead cells). In this case all other
482 methods do not work correctly, because their assumptions are violated (Fig. 6). Note however that an
483 important drawback of this method is that the chosen threshold value is arbitrary and may have no
484 biological meaning.

485 THE MAX GROWTH ACCELERATION is a very elegant method from mathematical point of view, and it
486 may be a good choice for growth curves with non-standard shapes. However, it is very sensitive to
487 noise (i.e. the calculation of the second derivative is very noise sensitive, Fig. 5). We recommend
488 using smoothening function before applying the max growth acceleration method (Fig. 6).

489 The most popular TANGENT METHOD works reasonably well even if the assumption about the constant
490 growth rate is violated. Additionally, it is not highly affected by data noisiness, but it performs worse
491 than the parameter fitting method if the measurements are not taken often enough (Fig. 5). The
492 challenging step may be the choice of how to draw the tangent line. If the tangent line is drawn to one
493 point only (the point where the growth rate is maximal) there is a risk its slope will be under or
494 overestimated if the data is noisy and an outlying point is chosen. This problem can be mitigated by
495 drawing the regression line around points in the exponential phase. However, it may be not obvious in
496 which time range the population grows exponentially. In fact, in order to know where the exponential
497 phase starts one needs to know where the lag phase finishes, which brings us back to the original
498 problem. Thus, the selection of data points in exponential phase often requires some manual inspection
499 or additional assumptions. Within our web tool, N points are chosen around the point with the
500 maximal growth rate, where N is a user-specified parameter. Note that the tangent method requires the
501 initial number of cells capable of proliferating (N_0) to be determined with high confidence. If a
502 substantial fraction of the population is dead or senescent, what may be the case for populations that
503 had previously experienced some stress (e.g. drug exposure, long-term starvation) [19,36], the N_0
504 captured by absorbance will be heavily overestimated.

505 THE PARAMETER FITTING TO THE LOGISTIC MODEL is the most robust lag calculation method. It shows
506 good accuracy even for noisy data (Fig. 5), and it can be used to overcome some technical limitations
507 (such as N_0 below detection level, or a high level of noise). Importantly, the method performed well
508 not only for the curves simulated from logistic model, but also for the ones simulated from Monod
509 model (Supplementary Fig. 4). The performance of this method depend on the shape of the growth
510 curve, e.g. if the growth curve highly deviates from the standard shape, the fitting may not converge to
511 any solution (Supplementary Fig. 5). This problem can be fixed by finding a more suitable
512 optimisation algorithm, initial parameter values, or data transformation. These options are available
513 within our web tool LAG PHASE DURATION CALCULATOR. However, we highlight the fact that the lag
514 phase duration estimation is dependent not only on the selected method but also on multiple
515 parameters of that method which tend to be underreported within experimental studies.

516

517 CONCLUSIONS

518 The results presented here emphasize that while determining lag phase duration, all steps (pre-
519 processing, choice of a method, and parameters) influence the final outcome. We would like to
520 highlight that all these steps should be thoughtfully reported to ensure data reproducibility and
521 credibility. Even the simplest tangent method requires specifying some details such as (i) if the initial
522 biomass is represented by the first measurement or the minimal value, or (ii) the number of data points
523 (or time frame) taken to draw the tangent line - whether a single point (e.g. [23]) or multiple points
524 from the exponential phase (e.g. [7]) were used.

525 Within this publication, we came out with two solutions to facilitate the process of reproducible lag
526 phase duration determination. First, we designed a decision tree (Fig. 7), which helps to choose the
527 method best suited to one's experimental conditions, taking into account various technical limitations
528 and data imperfections. Second, we have developed an online tool, which will help to directly compare
529 the lag phase duration estimated by different algorithms (i.e. combinations of methods, parameters,
530 and data pre-processing techniques). The tool allows parameter adjustments and data pre-processing.
531 Moreover, we share our code on GitHub
532 [https://github.com/bognabognabogna/microbial_lag_calulator] so that it can be further developed and
533 customised. In particular, we share the function "Calculate.Lag" which can be taken directly to the R
534 environment. We perceive our tool as an initial point to further improvements made by the scientific
535 community so that any new potential challenges can be solved in a reproducible way.

536

537 METHODS

538 EXPERIMENTAL GROWTH CURVES:

539 The empirical growth curve data used here were a part of a project described in Opalek *et al.* (2022)
540 [19]. All growth curves were acquired by growing *Saccharomyces cerevisiae* S288C cultures in rich
541 YPD media at 30°C. The populations were starved in various conditions before the growth procedure
542 (see details in Supplement). The populations' densities were monitored by absorbance measurements
543 (optical density (OD), 600 nm in SpectraMax iD3) taken every half an hour. Then, the biomass was
544 calculated according to the equations:

545 For OD measurements below 0.1: $10^{(1.885845 + 28.72096 \times \text{OD})}$

546 For OD measurement equal or above 0.1: $3566518 \times \text{OD} + 26754296 \times \text{OD}^2 - 19881567 \times \text{OD}^3$

547 SIMULATED GROWTH CURVES:

548 Growth curves shown in Fig. 1 were simulated from the models described in the Supplement, and for
549 time points spanning every 6 minutes between 0 and 24 hours. The parameters used are listed in the
550 Supplementary Table 3.

551 LAG DURATION CALCULATION METHODS:

552 Let t denote time, λ denote lag duration, B denote biomass, and let t_i denote the i 'th time point of the
553 growth curve. If we define $N = \ln(B)$, then $\frac{dN}{dt}$ can be understood as the growth rate.

554 Additionally let B_0 denote the first observation of biomass, and $N_0 = \ln(B_0)$

555 **Tangent to max. growth line**

556 The derivative of $\ln N$ is approximated using to the central scheme i.e.

$$557 \quad \frac{dN(t_i)}{dt} = \frac{N(t_{i+1}) - N(t_{i-1}))}{t_{i+1} - t_{i-1}}$$

558 Then the maximal growth rate is defined as the maximum value of $\frac{dN}{dt}$ found within the growth curve

559 i.e.: $\max_i \left(\frac{dN(t_i)}{dt_i} \right)$. The first point at which growth rate is maximal is then denoted as $(t^{\max.growth},$

560 $N^{\max.growth}$). Finally, a tangent line to this point is calculated.

561 Subsequently, lag duration is defined as the time when that tangent line crosses the N_0 line. This value
562 can be calculated as:

$$563 \quad \lambda = (N_0 - N^{\max.growth} - \max_i \left(\max_i \left(\frac{dN(t_i)}{dt_i} \right) \right) * t^{\max.growth}) / \max_i \left(\frac{dN(t_i)}{dt_i} \right)$$

564 **Tangent to max. growth point**

565 The first point at which growth rate is maximal is calculated as above and it is denoted as
566 $(t^{\max.growth}, N^{\max.growth})$. Then n points around that point are taken and a regression line is
567 calculated using the *lm* function from the *stats* package (R). Subsequently, lag duration is defined as
568 the time when that regression line crosses the N_0 line. Within the manuscript $n = 3$. However, within

569 our web tool this value can be modified by the user. Moreover, the value of N_0 can be defined either as
570 the first or the minimal $\log(\text{biomass})$ value.

571 **Parameter fitting to logistic model**

572 All parameters of the logistic model (described in Supplement) are fitted simultaneously to the growth
573 curve data using the *nlsLM* function from *minpack.lm* package (R), and the Levenberg-Marquardt
574 algorithm, `max.iter = 100`. The initial values are estimated from the data and the following initial
575 values: initial $K = \max(B)$, and initial lag = lag as calculated with the tangent method, and the initial
576 growth rate is fitted to the data points that are likely to be in exponential growth i.e. those where
577 biomass is between $B_0 + 0.2(\max(B) - B_0)$ and $B_0 + 0.8(\max(B) - B_0)$. All these initial values
578 can be adjusted within the web tool.

579 **Parameter fitting to Baranyi model**

580 All parameters of the Baranyi and Roberts model (described in Appendix) are fitted simultaneously to
581 the growth curve data using the *nls* function from *stats* package (R) and the *baranyi* formula from the
582 *nlsMicrobio* package. We use the Gauss-Newton algorithm, `max.iter = 100`, and the following initial
583 values: `init.LOG10Nmax = $\max(\log_{10}(B))$` , `init.LOG10N0 = $\log_{10}(B_0)$` , and the initial growth rate is
584 fitted to the data points that are likely to be in exponential growth i.e. those where biomass is between
585 $B_0 + 0.2(\max(B) - B_0)$ and $B_0 + 0.8(\max(B) - B_0)$. All these values can be adjusted within the
586 web tool.

587 **Max. growth acceleration**

588 The second derivative of N is calculated approximated with the central scheme i.e.

$$589 \quad \frac{d^2N(t_N)}{dt^2} = \frac{N(t_{N+1}) + N(t_{N-1}) - N(t_N)}{((t_{N+1} - t_{N-1})/2)^2}$$

590 Then the max. growth acceleration point is defined as the maximum value of $\frac{d^2N(t_i)}{dt^2}$ found within the
591 growth curve i.e.: $\max_i(\frac{d^2N(t_i)}{dt^2})$. Consequently, lag duration λ is defined as the minimum time t_M at
592 which $\frac{d^2N(t_i)}{dt^2} = \max_i(\frac{d^2N(t_i)}{dt^2})$.

593 **Biomass increase**

594 Let us define:

$$595 \quad \Delta B_{t_i} = B(t_i) - B_0$$

596 Lag duration λ is defined as the minimum time t_M at which

$$597 \quad \Delta B_{t_M} \geq \text{threshold}$$

598 Finally, if the lag calculated by any of the method above turn out negative (which indeed may happen
599 in the tangent and parameter fitting methods) we assume it is equal to 0.

600 Throughout this manuscript `threshold = 105`. However, within our web tool this value can be modified
601 by the user. Moreover, the value of B_0 can be defined either as the first or the minimal biomass value.

602 Additionally in case the lag estimate is negative, NA is returned.

603 **The code used to calculate the lag according to various methods can be found on GitHub**
604 **https://github.com/bognabognabogna/microbial_lag_calculator**

605

606 ACKNOWLEDGMENTS

607 We would like to thank Wolfram Moebius, Ryszard Korona, Joanna Rutkowska, Aleksandra Walczak,
608 Hanna Tutaj and Adrian Piróg for the discussion and their valuable comments. The research was
609 funded by the Priority Research Area BioS under the program Excellence Initiative – Research
610 University at Jagiellonian University in Krakow to BJS; by the Polish National Agency of Academic
611 Exchange, grant number PPN/PPO/2018/00021/U/00001 to BJS, the programme “Excellence
612 Initiative–Research University” at the Jagiellonian University in Kraków, Poland (grant number
613 UIU/W18/NO/28.07) to MO; the National Science Centre, Poland, the OPUS grant to D.W.-S. (grant
614 number 2017/25/B/NZ8/01035); the Biology Department research subsidies (grant number
615 N18/DBS/000019 to MO and DWS).

616

617 AUTHOR CONTRIBUTION

618 Conceptualization M.O., B.J.S., D.W.-S.; Empirical data M.O.; Data visualization B.J.S., M.O.; B.J.S.
619 developed the web server MICROBIAL LAG PHASE DURATION CALCULATOR; Writing-
620 original draft preparation - M.O, B.J.S.; Writing - reviewing B.J.S., D.W.-S.

621 All authors have read and agreed to the published version of the manuscript

622

623 CONFLICT OF INTEREST

624 The authors declare no conflict of interest.

625

626 REFERENCES

- 627 1. Müller M. Ueber den Einfluss von Fiebertemperaturen auf die Wachstumsgeschwindigkeit
628 und die Virulenz des Typhusbacillus. *Zeitschrift für Hyg und Infect.* 1895;20: 245–280.
629 doi:10.1007/BF02216656
- 630 2. Brejning J, Jespersen L, Arneborg N. Genome-wide transcriptional changes during the lag
631 phase of *Saccharomyces cerevisiae*. *Arch Microbiol.* 2003;179: 278–294. doi:10.1007/s00203-
632 003-0527-6
- 633 3. Brejning J, Arneborg N, Jespersen L. Identification of genes and proteins induced during the
634 lag and early exponential phase of lager brewing yeasts. *J Appl Microbiol.* 2005;98: 261–271.
635 doi:10.1111/j.1365-2672.2004.02472.x
- 636 4. Brejning J, Jespersen L. Protein expression during lag phase and growth initiation in
637 *Saccharomyces cerevisiae*. *Int J Food Microbiol.* 2002;75: 27–38. doi:10.1016/S0168-
638 1605(01)00726-7
- 639 5. Rolfe MD, Rice CJ, Lucchini S, Pin C, Thompson A, Cameron ADS, et al. Lag phase is a
640 distinct growth phase that prepares bacteria for exponential growth and involves transient metal
641 accumulation. *J Bacteriol.* 2012;194: 686–701. doi:10.1128/JB.06112-11
- 642 6. Bertrand RL. Lag Phase Is a Dynamic, Organized, Adaptive, and Evolvable Period That
643 Prepares Bacteria for Cell Division. Margolin W, editor. *J Bacteriol.* 2019;201: 1–21.
644 doi:10.1128/JB.00697-18
- 645 7. Jasnos L, Tomala K, Paczesniak D, Korona R. Interactions between stressful environment and
646 gene deletions alleviate the expected average loss of fitness in yeast. *Genetics.* 2008;178:
647 2105–2111. doi:10.1534/genetics.107.084533
- 648 8. Reding-Roman C, Hewlett M, Duxbury S, Gori F, Gudelj I, Beardmore R. The unconstrained
649 evolution of fast and efficient antibiotic-resistant bacterial genomes. *Nat Ecol Evol.* 2017;1:
650 0050. doi:10.1038/s41559-016-0050
- 651 9. Hamill PG, Stevenson A, McMullan PE, Williams JP, Lewis ADR, Sudharsan S, et al.
652 Microbial lag phase can be indicative of, or independent from, cellular stress. *Sci Rep.*
653 2020;10: 1–20. doi:10.1038/s41598-020-62552-4
- 654 10. Adkar B V., Manhart M, Bhattacharyya S, Tian J, Musharbash M, Shakhnovich EI.
655 Optimization of lag phase shapes the evolution of a bacterial enzyme. *Nat Ecol Evol.* 2017;1:
656 1–6. doi:10.1038/s41559-017-0149
- 657 11. Fridman O, Goldberg A, Ronin I, Shoresh N, Balaban NQ. Optimization of lag time underlies

- 658 antibiotic tolerance in evolved bacterial populations. *Nature*. 2014;513: 418–421.
659 doi:10.1038/nature13469
- 660 12. Jomdecha C, Prateepasen A. Effects of pulse ultrasonic irradiation on the lag phase of
661 *Saccharomyces cerevisiae* growth. *Lett Appl Microbiol*. 2011;52: 62–69. doi:10.1111/j.1472-
662 765X.2010.02966.x
- 663 13. D’Elia R, Allen PL, Johanson K, Nickerson CA, Hammond TG. Homozygous diploid deletion
664 strains of *Saccharomyces cerevisiae* that determine lag phase and dehydration tolerance. *Appl*
665 *Microbiol Biotechnol*. 2005;67: 816–826. doi:10.1007/s00253-004-1793-1
- 666 14. Vermeersch L, Perez-Samper G, Cerulus B, Jariani A, Gallone B, Voordeckers K, et al. On the
667 duration of the microbial lag phase. *Curr Genet*. 2019;65: 721–727. doi:10.1007/s00294-019-
668 00938-2
- 669 15. Cerulus B, Jariani A, Perez-Samper G, Vermeersch L, Pietsch MJ, Crane MM, et al.
670 Transition between fermentation and respiration determines history-dependent behavior in
671 fluctuating carbon sources. *Elife*. 2018;7. doi:10.7554/eLife.39234
- 672 16. Bheda P. Metabolic transcriptional memory. *Mol Metab*. 2020;38: 100955.
673 doi:10.1016/j.molmet.2020.01.019
- 674 17. Vriesekoop F, Pamment NB. Acetaldehyde addition and pre-adaptation to the stressor together
675 virtually eliminate the ethanol-induced lag phase in *Saccharomyces cerevisiae*. *Lett Appl*
676 *Microbiol*. 2005;41: 424–427. doi:10.1111/j.1472-765X.2005.01777.x
- 677 18. Pin C, Rolfe MD, Muñoz-Cuevas M, Hinton JCD, Peck MW, Walton NJ, et al. Network
678 analysis of the transcriptional pattern of young and old cells of *Escherichia coli* during lag
679 phase. *BMC Syst Biol*. 2009;3: 1–17. doi:10.1186/1752-0509-3-108
- 680 19. Opalek M, Smug B, Doebeli M, Wloch-Salamon D. On the Ecological Significance of
681 Phenotypic Heterogeneity in Microbial Populations Undergoing Starvation. Cuomo CA, editor.
682 *Microbiol Spectr*. 2022. doi:10.1128/spectrum.00450-21
- 683 20. Cerulus B, New AM, Pougach K, Verstrepen KJ. Noise and Epigenetic Inheritance of Single-
684 Cell Division Times Influence Population Fitness. *Curr Biol*. 2016;26: 1138–1147.
685 doi:10.1016/j.cub.2016.03.010
- 686 21. Opalek M, Wloch-Salamon D. Aspects of Multicellularity in *Saccharomyces cerevisiae* Yeast:
687 A Review of Evolutionary and Physiological Mechanisms. *Genes (Basel)*. 2020;11: 690.
688 doi:10.3390/genes11060690
- 689 22. Lee H-Y, Cheng K-Y, Chao J-C, Leu J-Y. Differentiated cytoplasmic granule formation in

- 690 quiescent and non-quiescent cells upon chronological aging. *Microb Cell*. 2016;3: 109–119.
691 doi:10.15698/mic2016.03.484
- 692 23. Moreno-Gámez S, Kiviet DJ, Vulin C, Schlegel S, Schlegel K, Doorn GS Van, et al. Wide lag
693 time distributions break a trade-off between reproduction and survival in bacteria. *Proc Natl*
694 *Acad Sci U S A*. 2020;117: 18729–18736. doi:10.1073/pnas.2003331117
- 695 24. Valík L, Šipošová P, Koňuchová M, Medved'ová A. Modelling the Effect of Temperature on
696 the Initial Decline during the Lag Phase of *Geotrichum candidum*. *Appl Sci*. 2021;11: 7344.
697 doi:10.3390/app11167344
- 698 25. Ranjbaran M, Carciofi BAM, Datta AK. Engineering modeling frameworks for microbial food
699 safety at various scales. *Compr Rev Food Sci Food Saf*. 2021;20: 4213–4249.
700 doi:10.1111/1541-4337.12818
- 701 26. Jindal S, Thampy H, Day PJR, Kell DB. Very rapid flow cytometric assessment of
702 antimicrobial susceptibility during the apparent lag phase of microbial (Re) growth. *Microbiol*
703 (United Kingdom). 2019;165: 439–454. doi:10.1099/mic.0.000777
- 704 27. Swinnen IAM, Bernaerts K, Dens EJJ, Geeraerd AH, Van Impe JF. Predictive modelling of the
705 microbial lag phase: A review. *Int J Food Microbiol*. 2004;94: 137–159.
706 doi:10.1016/j.ijfoodmicro.2004.01.006
- 707 28. Baty F, Flandrois JP, Delignette-Muller ML. Modeling the Lag Time of *Listeria*
708 *monocytogenes* from Viable Count Enumeration and Optical Density Data. *Appl Environ*
709 *Microbiol*. 2002;68: 5816–5825. doi:10.1128/AEM.68.12.5816-5825.2002
- 710 29. Baranyi J, Pin C. Estimating bacterial growth parameters by means of detection times. *Appl*
711 *Environ Microbiol*. 1999;65: 732–736. doi:10.1128/aem.65.2.732-736.1999
- 712 30. Fang T, Wu Y, Xie Y, Sun L, Qin X, Liu Y, et al. Inactivation and Subsequent Growth
713 Kinetics of *Listeria monocytogenes* After Various Mild Bactericidal Treatments. *Front*
714 *Microbiol*. 2021;12: 1–11. doi:10.3389/fmicb.2021.646735
- 715 31. Pierantoni DC, Corte L, Roscini L, Cardinali G. High-throughput rapid and inexpensive assay
716 for quantitative determination of low cell-density yeast cultures. *Microorganisms*. 2019;7.
717 doi:10.3390/microorganisms7020032
- 718 32. Baty F, Delignette-Muller ML. Estimating the bacterial lag time: Which model, which
719 precision? *Int J Food Microbiol*. 2004;91: 261–277. doi:10.1016/j.ijfoodmicro.2003.07.002
- 720 33. Liu Z, Fels M, Dragone G, Mussatto SI. Effects of inhibitory compounds derived from
721 lignocellulosic biomass on the growth of the wild-type and evolved oleaginous yeast

- 722 Rhodosporidium toruloides. *Ind Crops Prod.* 2021;170: 113799.
723 doi:10.1016/j.indcrop.2021.113799
- 724 34. Buchanan RL, Cygnarowicz ML. A mathematical approach toward defining and calculating the
725 duration of the lag phase. *Food Microbiol.* 1990;7: 237–240. doi:10.1016/0740-
726 0020(90)90029-H
- 727 35. Baty F, Delignette-Muller M-L. *nlMicrobio: data sets and nonlinear regression models*
728 *dedicated to predictive microbiology.* 2013.
- 729 36. Heinz J, Waajen AC, Airo A, Alibrandi A, Schirmack J, Schulze-Makuch Di. Bacterial Growth
730 in Chloride and Perchlorate Brines: Halotolerances and Salt Stress Responses of *Planococcus*
731 *halocryophilus*. *Astrobiology.* 2019;19: 1377–1387. doi:10.1089/ast.2019.2069
- 732 37. Murray JD. *Mathematical Biology.* Heidelberg: Springer Berlin, Heidelberg; 1989.
733 doi:<https://doi.org/10.1007/978-3-662-08539-4>
- 734 38. Verhulst P-F. Notice sur la loi que la population suit dans son accroissement. *Corresp*
735 *mathématique Phys.* 1838;10: 113–121.
- 736 39. Monod J. THE GROWTH OF BACTERIAL CULTURES. *Annu Rev Microbiol.* 1949;3: 371–
737 394. doi:10.1146/annurev.mi.03.100149.002103
- 738 40. Charlebois DA, Balázsi G. Modeling cell population dynamics. *In Silico Biol.* 2019;13: 21–39.
739 doi:10.3233/ISB-180470
- 740 41. Baranyi J, Roberts TA. A dynamic approach to predicting bacterial growth in food. *Int J Food*
741 *Microbiol.* 1994;23: 277–294. doi:10.1016/0168-1605(94)90157-0
- 742 42. Baranyi J, Roberts TA, McClure P. A non-autonomous differential equation to model bacterial
743 growth. *Food Microbiol.* 1993;10: 43–59. doi:10.1006/fmic.1993.1005
- 744 43. Hills BP, Wright KM. A new model for bacterial growth in heterogeneous systems. *Journal of*
745 *Theoretical Biology.* 1994. pp. 31–41. doi:10.1006/jtbi.1994.1085
- 746 44. McKellar RC. A heterogeneous population model for the analysis of bacterial growth kinetics.
747 *Int J Food Microbiol.* 1997;36: 179–186. doi:10.1016/S0168-1605(97)01266-X
- 748 45. Baranyi J. Comparison of stochastic and deterministic concepts of bacterial lag. *J Theor Biol.*
749 1998;192: 403–408. doi:10.1006/jtbi.1998.0673
- 750 46. Yates GT, Smotzer T. On the lag phase and initial decline of microbial growth curves. *J Theor*
751 *Biol.* 2007;244: 511–517. doi:10.1016/j.jtbi.2006.08.017
- 752 47. Takano S, Pawlowska BJ, Gudel I, Yomo T, Tsuru S. Density-dependent recycling promotes

- 753 the long-term survival of bacterial populations during periods of starvation. *MBio*. 2017;8: 1–
754 14. doi:10.1128/mBio.02336-16
- 755 48. Korolev KS, Xavier JB, Gore J. Turning ecology and evolution against cancer. *Nat Rev*
756 *Cancer*. 2014;14: 371–380. doi:10.1038/nrc3712
- 757 49. Goswami M, Bhattacharyya P, Tribedi P. Allee effect: the story behind the stabilization or
758 extinction of microbial ecosystem. *Arch Microbiol*. 2017;199: 185–190. doi:10.1007/s00203-
759 016-1323-4
- 760 50. Kim JY, Jeon EB, Song MG, Park SH, Park SY. Development of predictive growth models of
761 *Aeromonas hydrophila* on raw tuna *Thunnus orientalis* as a function of storage temperatures.
762 *Lwt*. 2022;156: 113052. doi:10.1016/j.lwt.2021.113052
- 763 51. Baranyi J, McClure PJ, Sutherland JP, Roberts TA. Modeling bacterial growth responses. *J Ind*
764 *Microbiol*. 1993;12: 190–194. doi:10.1007/BF01584189
- 765 52. Penfold WJ. On the Nature of Bacterial Lag. *J Hyg (Lond)*. 1914;14: 215–241.
766 doi:10.1017/S0022172400005817
- 767

768 SUPPLEMENT

769 FORMULATIONS OF MATHEMATICAL MODELS USED TO SIMULATE THE GROWTH CURVE DATA:

770 1. Exponential model

771
$$\frac{dN}{dt} = \begin{cases} rN, & t \geq L \\ 0, & t < L \end{cases}$$

772 which can be solved as

773
$$N(t) = \begin{cases} N(0)e^{r(t-L)}, & t \geq L \\ N(0), & t < L \end{cases}$$

774 where $N(t)$ is the population size at time t , L is the lag phase duration, and r is the growth rate
775 (constant in time).

776

777 2. Logistic model

778
$$\frac{dN}{dt} = \begin{cases} rN \left(1 - \frac{N}{K}\right), & t \geq L \\ 0, & t < L \end{cases}$$

779

780 where $N(t)$ is the population size at time t , L is the lag phase duration, r is the growth rate
781 (constant in time), and K is the saturation constant (i.e. the maximum population size).

782

783 3. Monod Model

784
$$\frac{dN}{dt} = \begin{cases} a \frac{VG}{K^G + G} N, & t \geq L \\ 0, & t < L \end{cases}$$

785

786
$$\frac{dG}{dt} = \begin{cases} -\frac{VG}{K^G + G} G, & t \geq L \\ 0, & t < L \end{cases}$$

787 where $N(t)$ is the population size at time t , $G(t)$ is the limiting nutrient (for example glucose)
788 concentration at time t , L is the lag phase duration. V denotes the maximal rate of the glucose
789 uptake pathway, and K^G denotes the Michaelis-Menten constant (so that if $K^G = G$, $\frac{VG}{K^G + G} = V/2$).

790 Moreover, the efficiency of converting glucose into biomass is described by a parameter a , which
791 for simplicity is assumed to be constant.

792 4. Baranyi and Roberts Model

793
$$\frac{dN}{dt} = r \left(1 - \frac{N}{K}\right) \frac{Q}{1 + Q} N$$

794
$$\frac{dQ}{dt} = vQ$$

795 Where $N(t)$ is the population size at time t , K is the saturation constant (i.e. the maximum
796 population size), and Q represents the physiological state proportional to the concentration of
797 some critical substrate.

798 THE GROWTH CURVE DATA:

799 Supplementary Table 1 gathers information about the populations used as examples (Fig. 2, Fig. 3) for
800 empirical growth curves within this publication (Fig. 2, 6). We choose growth curves that demonstrate
801 possible challenges in analysis, such as: biomass drop at the beginning of measurements (curve_1,
802 curve_6), prolonged lag phase (curve_7, curve_8, curve_11), lack of easily-visible lag phase
803 (curve_3), slow biomass increase (curve_8, curve_9), lack of exponential growth phase (curve_11),
804 turbulent measurements in biomass (curve_10).

805 The data was originally collected to analyse possible advantages of phenotypic heterogeneity within a
806 starving clonal population and it was used in Opalek *et al.* 2022. In particular, the growth curves come
807 from three artificially prepared *S.cerevisiae* population types: Q monoculture, NQ monoculture, and
808 mix culture. The Q (growth-arrested quiescent cells) and NQ (non-quiescent) cells are distinct
809 phenotypes that can be separated from the stationary phase population (Allen *et al.* 2006). The
810 populations had experienced starvation in complex (spent rich YPD medium) or simple (H₂O)
811 environments and had been regrown in rich media afterward for fitness analysis. For details, see
812 Opalek *et al.* 2022.

813 The data was not analysed nor visualised in the form presented in this publication.

814 Supplementary Table 1. The summary of starvation conditions, chronological age, and phenotypic
815 states of populations used to acquire growth curves analysed within this publication.

CURVE ID	STARVATION MEDIA	STARVATION DURATION	CELL TYPE
curve_1	complex environment	7 days	NQ monoculture
curve_2	complex environment	7 days	NQ monoculture
curve_3	complex environment	7 days	natural mix culture
curve_4	simple environment	14 days	NQ monoculture
curve_5	complex environment	14 days	Q monoculture
curve_6	complex environment	14 days	Q monoculture
curve_7	simple environment	35 days	NQ monoculture
curve_8	complex environment	35 days	NQ monoculture
curve_9	complex environment	42 days	NQ monoculture
curve_10	simple environment	42 days	Q monoculture
curve_11	simple environment	42 days	NQ monoculture

816

817

818 Supplementary Table 2. The summary of lag phase durations calculated by various methods
 819 (columns). The table compares the similarities of results for each of the curves. The numbers are given
 820 in hours.

821

CURVE_ID	BIOMASS INCREASE	MAX GROWTH ACCELERATION	PAR. FITTING TO THE BARANYI MODEL	PAR. FITTING TO THE LOGISTIC MODEL	TANGENT TO MAX GROWTH LINE	TANGENT TO MAX GROWTH POINT	AVERAGE \pm SD	MAX	MIN
curve_1	2	1.5	2.6	1.9	1.6	1.6	1.87 \pm 0.83	2.60	1.50
curve_2	1	1.5	2.6	1.9	1.6	1.6	1.70 \pm 1.40	2.60	1.00
curve_3	1	1.5	2	0.9	0.7	0.7	1.13 \pm 1.33	2.00	0.70
curve_4	3.5	3.5	6.1	5.2	4.4	4.4	4.52 \pm 5.07	6.10	3.50
curve_5	2	1	2.5	1.9	1.8	1.7	1.82 \pm 1.19	2.50	1.00
curve_6	2	1	2.5	2.2	1.9	1.9	1.92 \pm 1.27	2.50	1.00
curve_7	1.5	5	NA	11	8.5	8.5	6.90 \pm 54.70	11.00	1.50
curve_8	7	3	7.9	6.8	6.6	6.7	6.33 \pm 14.43	7.90	3.00
curve_9	4	1	5.6	4.1	4.5	4.4	3.93 \pm 11.95	5.60	1.00
curve_10	1	4	7.3	5.8	5.1	5.1	4.72 \pm 22.47	7.30	1.00
curve_11	14.5	1.5	20.2	17.6	18.2	18.2	15.03 \pm 236.77	20.20	1.50

822

823

824 Supplementary Table 3. Default parameters used to simulate data from models described in section
 825 FORMULATIONS OF MATHEMATICAL MODELS USED TO SIMULATE THE GROWTH CURVE DATA.

Parameter name	Default value
Growth rate r (exponential and Baranyi model)	0.1 [h^{-1}]
Max. growth rate r (logistic model)	0.25 [h^{-1}]
Carrying capacity K (logistic model)	$5 * 10^6$ [cells/mL]
Initial biomass N_0	10^6 [cells/mL]
Lag L in logistic, exponential, and Monod model	2.5 [h]
Initial physiological state in Baranyi model Q_0	3.52 [units]
Efficiency of substrate uptake in Monod model a	$3 * 10^5$ [cells/mmol substrate]
Maximal substrate uptake rate in Monod model V	$1.5 * 10^{(-5)}$ [mmol substrate / cells \times h]
Michaelis-Menten constant in Monod model K^G	300 [mmol substrate]

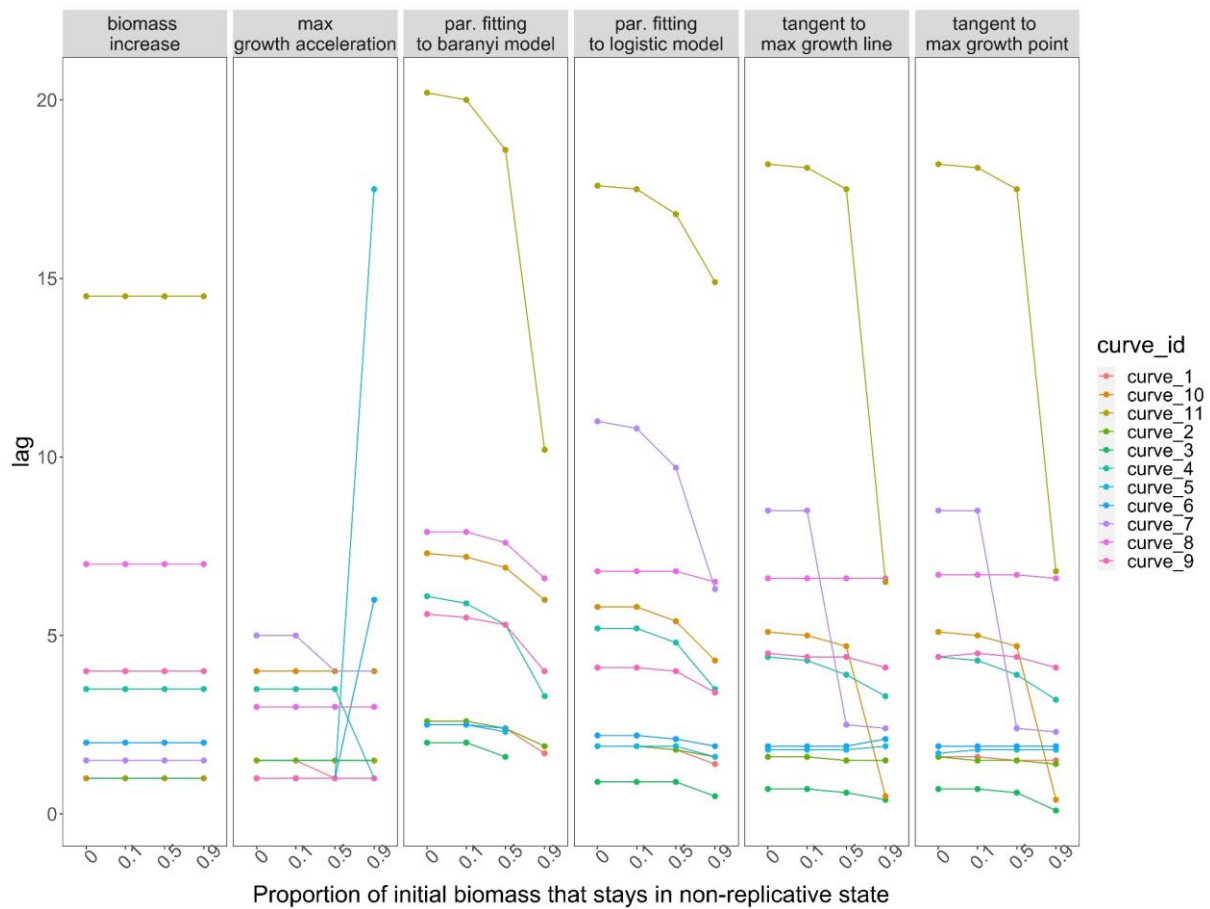
826

827

828

829

830



831

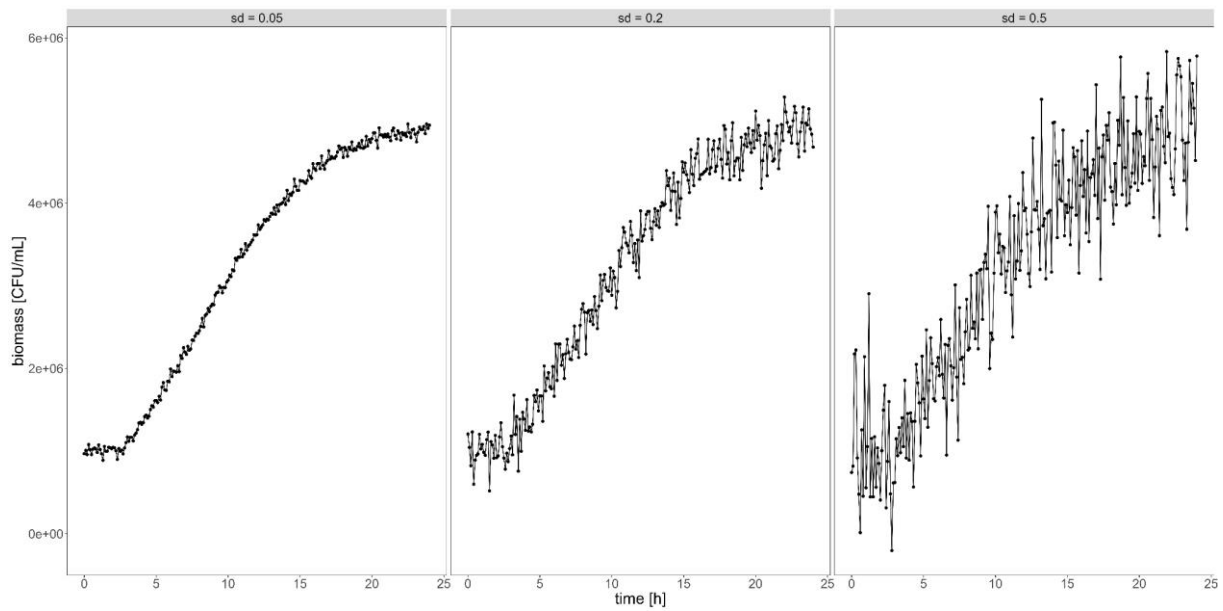
832 Supplementary Figure 1. Lag duration as calculated for 11 experimental growth curves with various
833 methods, assuming that a percentage of the initial population is non-replicative.

834 In case of growth curves, where there is no biomass increase for prolonged time (e.g. curve_11), the
835 proportion of alive vs senescent (permanently non-replicative cells) highly impact estimated lag
836 duration. If all cells are capable of proliferating ($x = 0$), then the observed lack of biomass increase is
837 indeed a lag phase, however if a substantial fraction of population is unable to proliferate ($x = 0.9$),
838 then the remaining 10% of alive cells start proliferate earlier (lag = 5-10 h, depending on the method
839 (columns)), however the increase in biomass is small to be marked as the lag phase end. That is why
840 the proportion of dead cells should be also monitored when analysing growth curves.

841

842

843



844

845

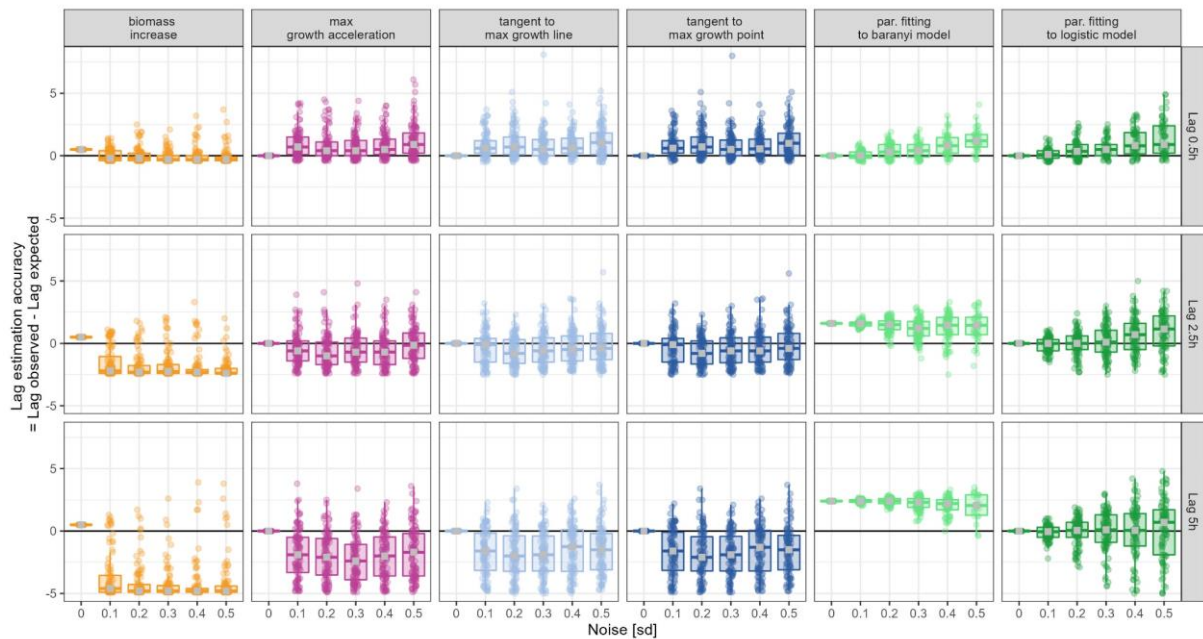
846 Supplementary Figure 2. The visualization of the impact of introduced noisiness (sd) on growth curve
847 shape. The noise was simulated from the random distribution with mean = 0 and standard deviation
848 standardized by the initial biomass B_0

849

850

851

852



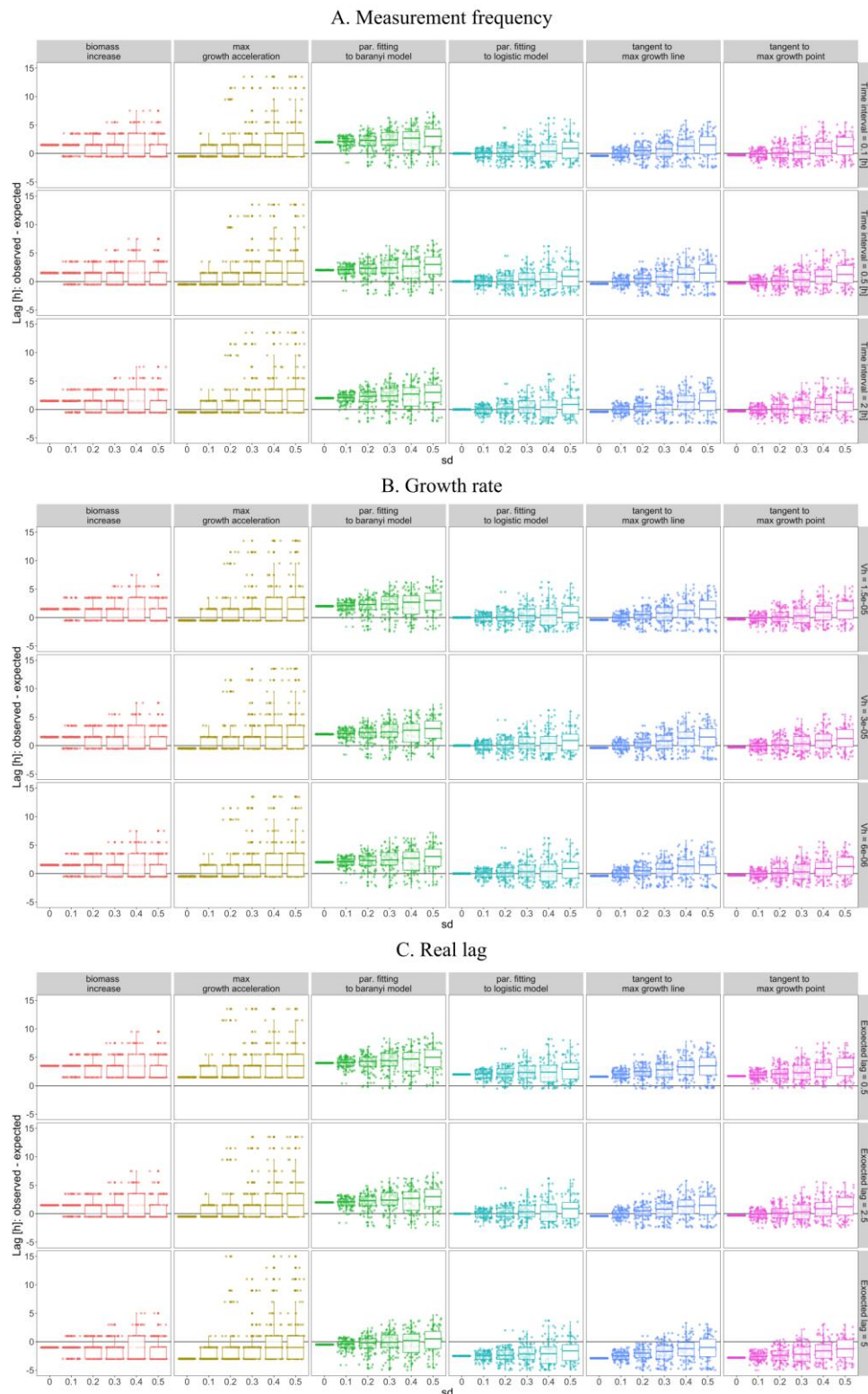
853

854 Supplementary Fig. 3. Impact of real lag phase duration on calculation accuracy. For each sd
855 (noisiness, x-axis), expected lag length (rows), and lag calculation method (columns), 100 simulations
856 were conducted (points). For each row, the true (expected) lag was set as a different value, e.g. in the
857 first row, the true lag was set as 0.5h, and the $y = 0$ correspond to lag = 0.5h, while in the second row,
858 $y = 0$ correspond to lag = 2.5h. Boxplots illustrate the distribution of points, and the median value
859 (grey square). All points located above $y = 0$, show these calculations where lag phase length was
860 overestimated, similarly, all points below $y = 0$ show calculations where lag duration was
861 underestimated.

862 Parameter fitting to Baranyi model systematically overestimates lag phase duration. For short lags
863 (first row), all but biomass increase methods tend to overestimate lag duration when noisiness
864 increase, while for long lags (last row), all but parameter fitting to logistic model methods
865 underestimate lag duration when noisiness increase. Median value (grey square) for the parameter
866 fitting to the logistic model is closest to $y = 0$ what indicates that this method is least biased.

867

868



869

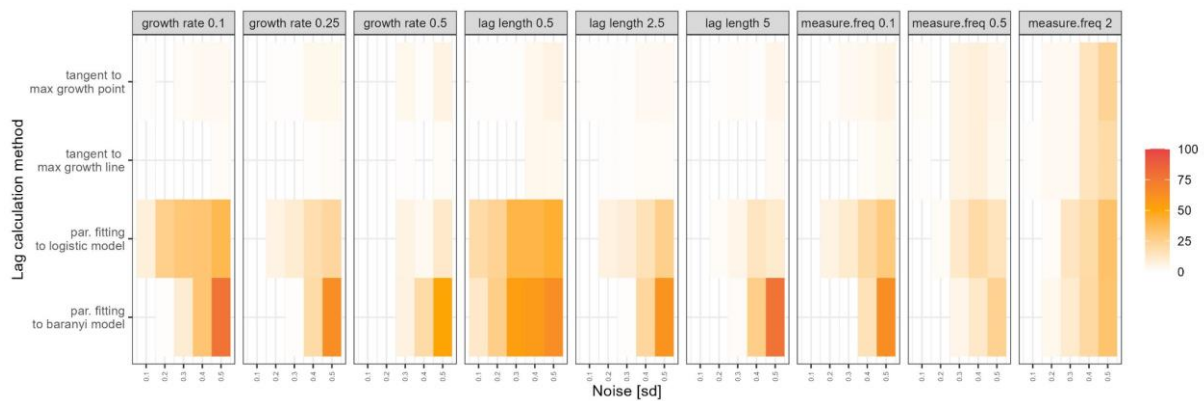
870 Supplementary Fig. 4. Testing robustness of results for data simulated via Monod model. The biases

871 and accuracies of the methods show the same pattern as described in the manuscript (Fig. 3, Fig. 4,

872 Supp. Fig. 3), and as such, the outcomes are not driven by the model itself.

873

874



875

876 Supplementary Fig. 5. Frequency of NA value generated (indicating failure of the lag estimation) out
877 of 100 simulated growth curves (the curves described in section: TESTING THE SENSITIVITY OF LAG
878 DETERMINATION METHODS TO DATA NOISINESS). In case of parameter fitting to model NA means that
879 the fitting didn't converge to any solution, while for tangent method NA is generated if lag was
880 estimated as a negative value. No filling indicates that all 100 lag estimations values were generated.
881 For biomass increase and max growth acceleration methods all lag estimations were successful and as
882 such they were excluded from the graph. The maximum of 78 failed lag estimations were generated
883 twice for parameter fitting to Baranyi model: for data simulated with slow growth rate (0.1) and long
884 lag phase (5h), both with and high noise (sd = 0.5).

885